

TECHNICAL MEMORANDUMS
NATIONAL ADVISORY COMMITTEE FOR AERONAUTICS

No. 883

University of Maryland
Glenn L. Martin College
of Engineering and Aero-
nautical Sciences
Library

DISTRIBUTION OF TEMPERATURES OVER AN AIRPLANE WING
WITH REFERENCE TO THE PHENOMENA OF ICE FORMATION

By Edmond Brun

Publications Scientifiques et Techniques
du Ministère de l'Air, No. 119, 1938

Washington
December 1938

NATIONAL ADVISORY COMMITTEE FOR AERONAUTICS

TECHNICAL MEMORANDUM NO. 883

DISTRIBUTION OF TEMPERATURES OVER AN AIRPLANE WING
WITH REFERENCE TO THE PHENOMENA OF ICE FORMATION*

By Edmond Brun

The most dangerous form of icing of an airplane occurs when it enters a cloud formed of surfused water droplets. The impact of the liquid droplets on the leading edges of the wings promotes a discontinuance of the metastable condition which determines the surfusion, and a layer of ice is formed rather quickly on the edges which may, in particularly severe cases, exceed 2 centimeters in thickness within 1 minute. At the same time, the icing continues to spread over the airplane, starting at the already-formed crystals.

The results obtained from the present study of temperature distribution over an airplane wing afford means for making the following statements as regards the conditions of ice accretion and the use of a thermic anti-icer or de-icer.

1. To begin with, it is obvious that ice can form on a wing only when the temperature is below or hovering around zero.** Since every part of the airplane has a higher temperature than that of the atmosphere, the cloud temperature must be below 0° in order to be able to promote freezing.

*"Répartition des températures sur une aile d'avion - Application aux phénomènes de givrage." Publications Scientifiques et Techniques du Ministère de l'Air, No. 119, 1938.

** However, it is pointed out that the hygroscopic state of a cloudy atmosphere can be below 1 (0.9, for example); the water deposited on the leading edge may evaporate in part, being accompanied by an absorption of 600 calories per gram, vaporized. Due to this fact, the temperature of the water, supposedly equal to 0.5° , for example, drops to 0° and freezes in part, since only 80 calories per gram of ice formed, is released. It is easily seen that the evaporation of a gram of water is accompanied by the freezing of about 7 grams of water.

(Continued on page 2.)

To illustrate: In the case of an airplane flying at 300 k.p.h. (186 m.p.h.), the atmospheric temperature should be below about -1.5° . In level flight and at an atmospheric temperature of -2° , ice forms only on the upper surface of the wings; observations, moreover, confirm that for the cases of ice formation obtained at much higher temperatures, it is largely confined to the upper surfaces of the wings.

Objections to the foregoing may be voiced that numerous cases of ice accretions have been recorded at 0° temperature but, let us remark, the so-called "atmospheric temperature" was read on a strut thermometer subjected to the same causes of heating as the airplane itself, so that the temperature of the cloud was certainly lower than that recorded.*

2. The thermic effects produced on contact of the air with the moving wing rather oppose ice accretion; this is one of the rare cases when the reduced energy produced during a motion is able to serve some purpose. Since the differences in temperature between the various points of the airplane and atmosphere increase substantially as the square of the speed, an increase in airplane speed should lower the frequency of ice-formation cases. Thus, on very fast airplanes - say, of 500 k.p.h. (310 m.p.h.) - no ice will accumulate on certain parts of the wing unless the ambient temperature is -4.5° .**

(Continuation of footnote from previous page)

This explains why, in a foggy and nonsaturated atmosphere, incidences of icing may be observed on airplane wings at above 0° temperature (in particular, Rebuffet's observations in the Chalais-Meudon wind tunnel). In the following, it is assumed that the hygroscopic state of the freezing cloud is 1 and, consequently, that no ice accretion is observed on a wing unless the temperature is at least 0° .

*Furthermore, according to the previous footnote, if the hygroscopic state of the atmosphere is below 1, the ice accretion may occur at higher temperatures than previously indicated, but these temperatures are always lower than those prevailing if the thermal effects due to friction, did not intervene.

**These conclusions are based on the data from heat measurements of bodies moving in air; the mathematical results will probably be a little different for bodies moving in fog, but the qualitative conclusions will be the same in both cases.

3. The thermic procedure in the fight against ice accretion on the wing consists in electrical heating of the leading edge, and the most promising method seems to be that which consists in covering the outside of the leading edge with a superficial resistance.

The dangerous cases of ice formation generally occur at atmospheric temperatures above -8° , that is, at wing temperatures a few degrees below 0. In order to maintain, in flight, the leading-edge temperature a little above 0, or in other words, for the anti-icing, the electric power input does not seem to be great: around 0.5 kilowatt per square meter at -1° , and at a 300 k.p.h. (186 m.p.h.) speed.

The effect of airplane speed on the effectiveness of the de-icer is largely dependent upon conditions of usage. A speed increase has a twofold thermic effect: first, the coefficient of convection increases, which tends to lower the temperature (proportional to the speed); then the friction increases, which tends to raise the temperature (proportional to the square of the speed).

The entire experimental study of the operation of a Badin antenna-type de-icer was made by Jampy, Lecardonnell, and the writer (*Revue Aéronautique Internationale*, no. 19, March 1936, p. 68). The results being qualitatively the same in the case of a leading edge, I believe a reproduction of the diagrams should prove of interest. Figure 1 shows the difference in temperature between the antenna and the air against the speed for a constant heating. It is readily seen on the curves how, starting at 300 k.p.h. speed, it is advantageous to lower or raise the speed in proportion as the heating of the experimental antenna corresponds to a power output of more or less than 16 watts. Figure 2 shows the electric power w necessary in the antenna plotted against speed, in order to keep the temperature difference between air and antenna constant. We believe that this power first increases with the speed, reaches a maximum, and then decreases. Figures 3 and 4 illustrate the effect of altitude on the temperature difference or the heating: high altitude favors operation of the de-icer.

4. It seems that the formation of ice on the wing ought to be accompanied by a temperature rise which brings the accretion to 0° ; for example, the discontinuance, on contact with the wing, of the surfusion of the liquid droplets at -6° should induce (if nothing else happened) the

water to freeze to 8 percent, while the solid-liquid mixture should reach 0° temperature. In fact, it is proper to remark that the saturation pressure of the ice-water mixture at 0° (or, to be more exact, at the temperature of the dripping point, itself very close to 0°) is higher than the saturation point of water superfused to -6° ; an evaporation, very much intensified by the wind, is therefore produced at the wing, which causes considerable freezing and may also lower the temperature if the ice happens to be dry.

All we can affirm is that, following a deposit of ice the temperature of the wing rises probably close to 0° under certain conditions.

5. If the thermic effects of friction favor the operation of the thermic anti-icer, the functioning of the de-icer is facilitated by the release of heat which accompanies the deposit of ice.

Suppose, for example, that the airplane flies in such a cold fog or mist that the electric power consumed by the electrical resistance which covers the leading edge of the wing is insufficient to provide a temperature above 0° : icing results. Since the wing heats up during the icing, the electric power consumed in the resistance will then allow of attaining more readily the melting temperature of the ice, and the de-icing will be followed by separation of the thin ice film that coats the wing. This phenomenon recurs periodically and prevents the formation of a big hump of ice on the wing. This is one method of operation of the electrical device which, like the anti-icer, prevents any deformation of the profiles even during very low weather. It ought to be possible to use it in the majority of cases without excessive power consumption.

6. Supposing that the electrical device does not function as outlined above - whether because the ice that forms maintains a low temperature or because the icing was not observed soon enough: Then, it is a question of separating the solid hump which covers the leading edge by creating a film of water between the wing and the ice within less than 2 to 3 minutes.

The convection no longer plays an essential part since the isolating layer of ice opposes an obstacle to thermal exchange between wing and atmosphere; a cursory calculation shows that 5 mm coating of ice should, on a fast airplane,

decrease the thermic exchanges with the atmosphere in the ratio of about 1:8 if the permanent regime is attained. It may therefore be supposed, especially when the regime is variable, that the wind of the airplane does not affect the temperature of a wing heated and coated with a heavy layer of ice, very much. This fact makes it possible to study the problem of de-icing on a wing at rest - that is, to say, in the wind tunnel. The following contains the essential data obtained from this study.

a) Figure 5 shows the curve giving the energy required (in kilo-joules) to separate the ice (subject to a very slight lift) from an area of 1 square meter, plotted against initial temperature of the iced surface. (During the separation, the surface is in a thermostat with initial temperature.) It is seen that the energy required for de-icing increases about 14 kilo-joules per square meter for 1° drop in initial temperature of the surface; in addition, the ordinate to the origin of the curve is also equal to about 14 kilo-joules: this is the amount of energy necessary for separating the ice at 0° (1 cv consumed during 19 seconds).* Thus in the case of -5° initial temperature, it requires five times more energy to bring the outer surface to 0° than to melt the adhering ice film. Obviously, this result is largely dependent upon the constitution of the wing, and much upon its thermic capacity as well as on the thickness of the ice. However, the value of the ordinate at the origin, 14 kilo-joules, is not affected by the constitution of the wing and the thickness of the ice, which gives this figure a certain value.**

b) When de-icing is effected during a variable period the energy input certainly has some bearing on it. To begin with, when nearly all the energy is supplied at the place where the actual effect is produced, it is of advan-

*This energy promotes the melting of about 42 grams of ice, and consequently, the formation of a film of water between the ice and the wing of around 1/20 mm thickness.

**The importance of the energy necessary for heating the wing emphasizes the interest of an outside heating of the wing, employed in our tests. The study of the heating curve shows, moreover, that the ice separates when the temperature of the inside wall is $-2t^{\circ}/5$, if the initial temperature is $-t^{\circ}$. On the contrary, with internal heating the inner surface must be brought above zero in order to assure separation. The gain in energy is therefore quite plain.

tage to increase the electrical power. Figure 6 shows - plotted against the power in kilowatts per square meter - the curve of the energy in kilojoules per square meter required to de-ice a surface, at -4° , coated with a 6 mm layer of ice. It is seen from this curve that, by supplying 3 kilowatts per square meter power, it requires an energy twice as small as with 1 kilowatt per square meter or, in other words, the ice separates six times faster in the first case than in the second (13 seconds instead of 83). This has made it seem to be of advantage to divide the surface to be de-iced into several sections which may be de-iced successively (each section including two symmetrical portions in relation to the axis of the airplane).

A. THEORETICAL STUDY OF TEMPERATURE DISTRIBUTION

ABOUT A SOLID MOVING IN A FLUID

I. Distribution of Speed Around an Obstruction

Visualize a cylindrical fluid jet of velocity v_0 (at infinity). When the fluid approaches an obstacle - say, an airplane wing, the velocity field ceases to be uniform. In a permanent regime and in the vicinity of a solid, it is necessary to consider the boundary layer where, as a result of the viscosity, the solid decelerates the fluid. The velocity of the fluid - zero at some points, M at the wall - increases rapidly when one describes the normal to the wall at point M ; it speedily reaches a value v that changes only very slowly and which is generally termed the "local velocity at point M of the profile." After velocity v has been reached, we are outside the boundary layer in the free fluid. The velocity v is only approximated because the change from boundary layer to free fluid is gradual; there certainly is no discontinuity in the velocity field.

In aerodynamics it is assumed that, outside of the boundary layer and the wake, the phenomena comply with the laws of perfect fluids. Another assumption is that, if the radius of curvature at point M is not very small, the pressure does not change in the boundary layer when displaced over the normal to point M ; the pressure is therefore the same at the wall and in the free fluid where the velocity is v . It is not necessary to discuss these assumptions since they are the basis of many wind-tunnel tests and constitute, very likely, a sufficient approximation for the calculations resorted to.

Now the problem of velocity distribution about an air-foil reduces to the measurement of the pressures at the wall, provided that for a perfect fluid the relation between the pressure p of the fluid at a point and its velocity v at that point, is known. The various assumptions which allow the formation of such a relationship are briefly summarized.

As first approximation, it is generally assumed that the pressure changes in the fluid are not accompanied by changes in volume or temperature and, consequently, by no change in internal energy - which is briefly expressed (perhaps a little too summarily) by saying that the fluid is "incompressible." The whole fluid flow can thus be considered as being isothermic; the exchange of heat within the fluid is zero and all passing phenomena are adiabatic. Under these conditions, the application of the energy-conservation principle to a fluid filament leads to Bernoulli's formula.

Consider a very thin filament which passes simultaneously at point A upstream from the obstruction, and point M of the wall. The velocity at point A is v_0 and the pressure is p_0 (defined by static tube); at point M the velocity is v and the pressure p . The outflow during the time interval Δt is Δm ; it occupies the constant volume ΔV_0 .

The principle of the conservation of energy is:

$$p \Delta V_0 + \frac{1}{2} \Delta m v^2 = p_0 \Delta V_0 + \frac{1}{2} \Delta m v_0^2$$

or, if ρ_0 is the constant specific fluid mass

$$\frac{p}{\rho_0} + \frac{1}{2} v^2 = \frac{p_0}{\rho_0} + \frac{1}{2} v_0^2 \quad (1)$$

and the equation of the velocity v at point M is:

$$v^2 = v_0^2 + 2 \frac{p_0 - p}{\rho_0} \quad (2)$$

At high velocities the pressure changes become very significant, and it is impossible to suppose that they do not entail changes in volume or temperature. However, since the change in temperature with the pressure (and consequently with the velocity) is taken into account, it is

more difficult to grant that the transformations produced in an air filament are adiabatic; the adjacent filaments which have not the same velocity, have no longer the same temperature and heat exchanges produced among themselves.* Therefore, even the fluid is assumed to be compressible and expansible, we would simply obtain an approximate result by applying the principle of conservation of energy to a thermically isolated fluid filament: this second approximation forms the Saint-Venant and Wantzel formula.

Consider the air filament that passes through points A and M. If p_0 is the pressure, ρ_0 , the specific weight, T_0 , absolute temperature, and U_0 , internal specific energy of the fluid at point A, where the velocity is v_0 , and if p , ρ , T , and U are the corresponding quantities at point M where the velocity is v , the principle of the conservation of energy allows us to write:

$$p \Delta V + \frac{1}{2} \Delta m v^2 + \Delta m U = p_0 \Delta V_0 + \frac{1}{2} \Delta m v_0^2 + \Delta m U_0$$

or

$$\frac{p}{\rho} + \frac{1}{2} v^2 + U = \frac{p_0}{\rho_0} + \frac{1}{2} v_0^2 + U_0 \quad (3)$$

Without incurring any greater errors than those introduced by the approximations so far, the air can be considered as a perfect gas, so that:

$$\frac{p}{\rho} = (c_p - c_v) T; \quad U = c_v T$$

Equation (3) then becomes:

$$c_p T + \frac{1}{2} v^2 = c_p T_0 + \frac{1}{2} v_0^2 \quad (4)$$

whence

$$v^2 = v_0^2 + 2c_p T_0 \left(1 - \frac{T}{T_0}\right)$$

The velocity-pressure relation is established by expressing the value of T/T_0 with the aid of the relation which ties the pressure to the temperature in the isentropic expansion of a perfect gas:

*Tremblot (Report no. 10 of this series) established equal velocity, hence equal temperature in adjacent filaments of the same section. The heat exchange consequently is insignificant. This holds true even more near obstructions, where the velocities in the same section are no longer equal.

$$\frac{T}{T_0} = \left(\frac{p}{p_0}\right)^{\frac{c_p - c_v}{c_p}}$$

It is, according to the Saint-Venant and Wantzel formula:

$$v^2 = v_0^2 + 2c_p T_0 \left[1 - \left(\frac{p}{p_0}\right)^{\frac{c_p - c_v}{c_p}} \right] \quad (5)$$

On comparing the results by Bernoulli's formula (first approximation) with those by the Saint-Venant and Wantzel formula (second approximation), the discrepancy will not exceed 1 percent for velocities below 100 meters per second. At low velocities equation (2) or equation (5) can be used for computing the velocity v , starting with pressure p .

II. Distribution of Temperatures Around an Obstacle

Saint Venant's formula in the form of equation (4) gives the relation between the velocity of the fluid at a point and its temperature as

$$\frac{v^2}{2} + c_p T = \frac{v_0^2}{2} + c_p T_0 \quad (4)$$

or, if the value of the velocity is replaced by its expression in function of the pressure (equation (5)):

$$c_p T + \frac{c_p}{c_p - c_v} \frac{p_0}{\rho_0} \left[1 - \left(\frac{p}{p_0}\right)^{\frac{c_p - c_v}{c_p}} \right] = c_p T_0$$

whence

$$T - T_0 = - \frac{p_0}{\rho_0 (c_p - c_v)} \left[1 - \left(\frac{p}{p_0}\right)^{\frac{c_p - c_v}{c_p}} \right]$$

$$\text{or} \quad T - T_0 = - T_0 \left[1 - \left(\frac{p}{p_0} \right)^{\frac{c_p - c_v}{c_p}} \right] \quad (6)$$

Equation (6) thus affords the possibility of knowing the temperature distribution in an air filament which winds around an obstacle by measuring the pressure on the obstacle.

A simpler expression for temperature T at point M can be obtained from an exchange of the velocity v , in equation (4), for its value by Bernoulli's formula (equation (1)): Then

$$-\frac{p}{\rho_0} + c_p T = -\frac{p_0}{\rho_0} + c_p T_0$$

where

$$T - T_0 = -\frac{1}{\rho_0 c_p} (p_0 - p) \quad (7)$$

or

$$T - T_0 = - T_0 \left(\frac{c_p - c_v}{c_p} \right) \left(1 - \frac{p}{p_0} \right) \quad (7 \text{ bis})$$

It may seem illogical to resort to both Bernoulli's and Saint Venant's formulas in establishing formula (7), but this contradiction appears only at low velocities, as we have seen that the two expressions of the velocity yield practically the same result. In the case of $p/p_0 = 0.95$, corresponding to a velocity change of the order of 100 meters per second, equations (6) and (7) give results differing scarcely 2 percent. Moreover, equation (7 bis) follows directly from equation (6) and is, we assume, p/p_0 near to 1 (i.e., $p-p_0$ small before p_0).

III. Distribution of Temperatures Over the Wall of an Obstruction

The numerous measurements made on the thermic phenomena produced by the displacement of a solid in fluid (cf. report No. 63 of this series) have led us to state that

the temperature θ of a point M on the wall is higher as the temperature T of the free fluid is closer. The temperature difference $(\theta - T)$ existing between the two edges of the boundary layer depends upon the viscosity and the thermal conductivity of the fluid, but practically little on the wall; particularly, the radius of curvature of this wall does not intervene. If v is the relative speed of the solid and of the free fluid at point M, we may write:

$$\theta - T = A v^2 \quad (8)$$

where A is a constant for a fluid under certain conditions. For air near normal conditions and speed in centimeters per second, the constant A is close to $4 \cdot 10^{-8}$.

To find the temperature difference $(\theta - T)$ at various points of the profile, simply replace in equation (8) the relative speed by its value given in equation (5):

$$\theta - T = A \left\{ v_0^2 + 2c_p T_0 \left[1 - \left(\frac{p}{p_0} \right)^{\frac{c_p - c_v}{c_p}} \right] \right\} \quad (9)$$

If restricted to the range of low speeds (below 100 m/s), Bernoulli's more simple equation can be used, whence:

$$\theta - T = A \left[v_0^2 + 2 \frac{(p_0 - p)}{\rho_0} \right] \quad (10)$$

Now we understand the process of the passage of temperature T of the far-off fluid to the temperature θ of point M of the solid in the fluid flow. The first temperature change $T - T_0$ is the result of the adiabatic compression, and the expansions around the obstacles; during these pressure changes the fluid is considered perfect and the changes are reversible. The second temperature change becomes manifest at the time of traversing the boundary layer; here the viscosity intervenes and the thermic effect is by nature largely irreversible. We express the temperature difference as:

$$\theta - T_0 = (\theta - T) + (T - T_0) \quad (11)$$

with allowance for the compressibility of the fluid (equations (6) and (9)):

$$\theta - T_0 = -T_0 \left[1 - \left(\frac{p}{p_0} \right)^{\frac{c_p - c_v}{c_p}} \right] +$$

$$+ A \left\{ v_0^2 + 2c_p T_0 \left[1 - \left(\frac{p}{p_0} \right)^{\frac{c_p - c_v}{c_p}} \right] \right\}$$

or

$$\theta - T_0 = Av_0^2 + T_0 \left[1 - \left(\frac{p}{p_0} \right)^{\frac{c_p - c_v}{c_p}} \right] (2c_p A - 1) \quad (12)$$

Assuming the fluid incompressible (equations (7) and (10)), it is:

$$\theta - T_0 = -\frac{1}{\rho_0 c_p} (p_0 - p) + A \left[v_0^2 + 2 \frac{(p_0 - p)}{\rho_0} \right]$$

or

$$\theta - T_0 = Av_0^2 + \frac{p_0 - p}{\rho_0} \left(2A - \frac{1}{c_p} \right) \quad (13)$$

A better comparison of the numerical values obtained by the two equations is afforded by replacing in equation (12) the value of the temperature T_0 by its expression

$$\frac{p_0}{\rho_0} (c_p - c_v).$$

$$\theta - T_0 = Av_0^2 + \frac{p_0 c_p}{\rho_0 (c_p - c_v)} \left[1 - \left(\frac{p}{p_0} \right)^{\frac{c_p - c_v}{c_p}} \right] \left(2A - \frac{1}{c_p} \right) \quad (12 \text{ bis})$$

This relation reduces to equation (13) in the particular case where p/p_0 approaches 1. Supposing $p/p_0 = 0.96$, which, for instance, is the case of a local velocity of 130 m/s with a velocity at infinity of 100 m/s; applied to equation (13), we find then:

$$\theta - T_0 = Av_0^2 + \frac{p_0}{\rho_0} \left(2A - \frac{1}{c_p} \right) 0.0400$$

and equation (12 bis) becomes:

$$\theta - \tau_0 = Av_0^2 + \frac{p_0}{\rho_0} \left(2A - \frac{1}{c_p} \right) 0.0406$$

Expressed in cm-g-s units, with $A = 4 \times 10^{-8}$, $\frac{p_6}{\rho_0} = \frac{10^9}{1.2}$, $c_p = 10^7$ ergs/gram, the values for the first case are 3.333° , and for the second, 3.323° . So long as $|(p/p_0) - 1|$ is less than 0.04, the absolute error does not exceed 1/100 of a degree. This condition was ordinarily complied with during the experiments related hereinafter.

However, if p/p_0 should become definitely different from 1, equation (12) is preferable. Suppose $\frac{p}{p_0} = 0.8$, which is the case of a local velocity of 210 m/s with a velocity at infinity of 100 m/s (customary in aviation); then equation (13) gives $+0.66^\circ$, while the more exact equation (12) gives $+0.55^\circ$, the error amounting to 0.16° .

IV. First Experimental Check

In report No. 63 (p. 67) of this series, equation (13) had been arrived at by a somewhat summary argument. We had figured, in the formula, the theoretical value of the constant A ($\eta/2k$).

Experiments made on 2 cm diameter cylinders (ch. VII, p. 57) led to a temperature-distribution curve, the shape of which agreed with that of the theoretical curve.

In view of the importance attaching to the knowledge of the temperatures on an airplane wing, it seemed practical to repeat the experimental measurements, first on a model wing, then on a full-sized wing. The advantage of these wind-tunnel tests over those made previously, is the concurrent determination of both the temperature and the pressure distributions.

B. EXPERIMENTAL LAY-OUT FOR STUDYING THE TEMPERATURE
DISTRIBUTION OVER AN AIRPLANE WING

I. Principle

To study the temperature distribution over a wing mounted in a wind tunnel, several metallic masses are distributed over an identical straight section, being built in flush in the insulating substance of the wing. Each one serves as a pressure tap, constituting one of the junctions of a copper-constantan thermocouple; the other junction is formed by a small cylinder R located in a part of the jet not disturbed by the wing.

During a measurement effected at a certain wind speed, all temperatures of the metallic masses are successively compared with those of the junction of R. In addition, by virtue of the disposition of junction R, if the temperature of the air entering the tunnel changes during the test, the temperature differences indicated by the thermocouples are not affected and it becomes useless to determine the air temperature exactly.

In a comparison of the theoretical and experimental results, the pressure distribution must be known. Hence, the wing was fitted with pressure orifices - symmetrical temperature orifices with respect to the plane of symmetry of the wing (fig. 7).

II. Original Arrangement

Mr. Lapresle, Chief Aeronautical Engineer, had placed at my disposal a Göttingen airfoil section No. 387, while I started to make a small model of it for preliminary testing in the small tunnel (1.80 m jet diameter) at Issy-les-Moulineaux.

This model, of solid wood, of 1.10 m span and 0.22 m chord, had 12 pressure and 12 temperature orifices as indicated in figures 7 and 8.

Each temperature orifice is fitted with a copper tap as presented in figure 9 (dimensions in tenths of millimeters), which fits flush in the wood, the surface AB be-

ing finished to give the smoothest possible wing surface. A 0.2 mm diameter copper wire and a 0.2 mm diameter constantan wire are soldered in the cavity C, both wires passing through the wing in a groove parallel to the generating lines; they emerge on the right side of the wing (fig. 10). At the point of emergence the 12 constantan wires are interconnected and joined to the constantan wire of the reference junction (visible below the wing in fig. 10). The difference in potential E, between the copper wire of, say, tap 2, and the copper wire of tap R, gives the difference in temperature between tap 2 and tap R (fig. 11).

The pressure taps are small hollow copper cylinders, of 0.5 mm diameter inside, and 3 mm diameter outside, set in the wing. The same grooves which, on the right side of the wing, serve for the copper and the constantan wires, are used on the left side for the 12 copper wires which allow the successive joining of the pressure leads to the manometer. The tubes are long enough to permit their connection with the rubber tubing outside of the air stream of the tunnel.

III. Second Arrangement

The equipment for the full-sized wing (5- by 1-meter) was made in the shop at Chalais-Meudon. The section with the pressure taps and the section with the temperature taps are symmetrical with respect to the plane of symmetry of the wing and 0.41 m away from it. The orifices, 13 in number, are divided over the top and bottom in the same way, as indicated in figure 12.

Each temperature tap, formed by a small piece of copper, is set into the wing; the wing being hollow, the fittings are somewhat different. The constantan wires soldered to the different pieces of copper, terminate at one point C inside the wing (fig. 13); between the tap and point C, all wires are of equal length (1 m), so that the resistances of the thermocouples will be the same. At this point C also terminates the constantan wire of the junction R, located outside the zone of influence of the wing. The difference in potential between the copper wire junction R and the copper wire of a tap - say, 2 - serves to measure the difference in temperature between tap 2 and junction R.

The pressure taps lead directly to a multiple manometer which allows the determination of every pressure at the same instant, by photography, while a manometric tube hooked to a pitot tube gives the speed at infinity v_0 at the same instant.

Figure 14 gives a view of the hook-up. The wing is mounted on a faired metal spindle and permits angle-of-attack changes. The copper wires of the thermocouples, as well as the rubber tubes leading to the manometer, pass through the flooring to the floor below, where the measurements are made.

IV. Temperature Recording

By connecting a galvanometer between the copper wire of junction R and that of the particular tap, a deflection is obtained which depends on the temperature differences between the two junctions (i.e., on the thermoelectric electromotive force) and on the total resistance of the circuit. This second variable can be eliminated with thermocouples having the same resistance and using the same length of constantan wire between junction R and each of the taps, and the same length of copper wire between the galvanometer and each tap. Naturally, the galvanometer itself is calibrated by means of a thermocouple identical with one of those used in the installation. A multiple switch installed as shown in figure 13, affords in a few minutes, the various temperature differences corresponding to divers taps. With the "Kipp" type galvanometer employed, it was easy to measure 0.01° .

With the first arrangement we had installed a compensating method for measuring the thermoelectric electromotive forces. In view of the timing factor involved in order that the comparison of temperatures at the different points reaches the wing in the same thermic stage, the installation of the opposition serves only to check from time to time, the results from the deflection method, employed in all measurements.

V. Pressure Recording

The manometer gives direct, the pressure difference $p - p_0$ between the tap to which it is connected and a

static tube located in the undisturbed jet. A pitot tube supplied the value $\rho_0 v_0^2/2$, where ρ_0 and v_0 are the specific weight and the speed in the undisturbed jet. It is recommended computing, for interpreting the results, the results $\frac{(p - p_0)}{(\rho_0 v_0^2/2)}$, which alone is figured in the tables.

C. MODEL TEST DATA

I. Principles of Measurements

The measurements were started in June 1936, in the small wind tunnel at Issy-les-Moulineaux.

Since it was possible to change the incidence of the wing in the air stream without stopping the tunnel, it was possible to effect, in permanent regime, a complete set of measurements (determination, at various incidences, of - 1) the wind speed; 2) the temperature at 12 points of the wing 3) the pressure at these same points). It is true that the incidence variation occasioned a concomitant change in wind velocity, but a slight action on the rheostat of the fan permitted of bringing the speed to a constant value (45 m/s).

It should not be necessary to repeat the results of more than one test series, since they are nearly all of the same degree of regularity.

II. Tabulation of Temperature-Recording Data

The incidence was measured with reference to the tangent to the lower wing surface (wall correction effected). Table I gives, for each incidence, the temperature at the various junctions, numbered from 1 to 12 (the temperature at junction R being counted as zero temperature). The number 1 corresponds to the junction at the leading edge; numbers 2, 3, 4, 5, 6, 7, and 8, to the junctions at the upper surface of the wing, counted from the nose toward the tail; numbers 9, 10, 11, and 12, to the junctions on the lower surface of the wing, counted from trailing toward leading edge. Figure 8 gives, at the same time, the position and number of junction.

TABLE I

Temperature tap	Incidence							
	-6.40°	-3.60°	-0.70°	+2.20°	+5°	+7.80°	+10.70°	+14.70°
1	0.51	0.69	0.95	0.98	1.00	1.02	0.91	0.73
2	1.01	.91	.92	.86	.77	.70	.60	.37
3	.82	.73	.74	.70	.58	.46	.45	.28
4	.88	.79	.67	.67	.65	.51	.48	.37
5	.76	.60	.61	.61	.59	.53	.48	.50
6	.74	.71	.72	.68	.68	.74	.69	.78
7	.79	.76	.86	.87	.83	.85	.85	.81
8	.91	.95	.96	.95	.95	.98	.94	.84
9	.94	.88	.92	.95	.86	.95	.91	1.01
10	.88	.85	.89	.89	.74	.83	.82	1.01
11	.85	.85	.92	.77	.74	.83	.82	1.01
12	.70	.79	.74	.77	.86	.89	.82	1.01

The rough result of the measurement for junction No. 4, for example, presents the temperature difference θ between junction 4 and that θ_0 of junction R. We easily pass from the difference $\theta - \theta_0$ to the difference between temperature θ of junction 4 and the temperature t_0 of the air in the air stream, by writing:

$$\theta - t_0 = (\theta - \theta_0) + (\theta_0 - t_0) \quad (14)$$

According to previous measurements (cf. Report No. 63 of this series) the temperature difference between a small solid conductor and the air, in relative displacement of velocity v_0 , substantially follows the equation $\theta_0 - t_0 = 4.2 \times 10^{-8} v_0^2$, with v_0 expressed in centimeters per second. For $v_0 = 4,500$ cm/s, it is $\theta_0 - t_0 = 0.85^\circ$ and, consequently:

$$\theta - t_0 = \theta - \theta_0 + 0.85^\circ \quad (14 \text{ bis})$$

These are the differences $\theta - t_0$ shown in table I. The four missing figures for junction 11 were due to an accident on the wires connecting the junction during the test.

III. Pressure Tables

The rough result of a pressure record is the pressure difference p at the particular tap and the static pressure p_0 in the undisturbed air stream. The pressure difference $p - p_0$ is measured with an alcohol manometer; the successive pressure measurements with the same manometer are easy since the pressure-tap tubes escape the air stream (fig. 10).

Inasmuch as it is the ratio of $p - p_0$ to the dynamic pressure $\rho_0 \frac{v_0^2}{2}$, which is of interest in the application of the formulas, this quantity $\frac{(p - p_0)}{(\rho_0 v_0^2/2)}$ is given in nondimensional form in table II. The value of $\rho_0 \frac{v_0^2}{2}$ is given direct by the pitot tube in the undisturbed flow.

TABLE II

Pressure tap	Incidence							
	-6.40°	-3.60°	-0.70°	+2.20°	+5°	+7.80°	+10.70°	+14.70°
1	-2.89	-1.24	0	+0.73	+0.98	+0.92	+0.55	+0.20
2	+.89	+.67	+.40	+.03	-.52	-1.12	-1.73	-2.62
3	+.25	-.10	-.49	-.94	-1.40	-1.95	-2.44	-3.15
4	-.10	-.41	-.76	-1.10	-1.45	-1.87	-2.27	-2.71
5	-.50	-.76	-1	-1.29	-1.51	-1.78	-1.97	-2.12
6	-.60	-.73	-.83	-.97	-1.04	-1.19	-1.19	-1.02
7	-.37	-.42	-.47	-.51	-.53	-.58	-.55	-.33
8	-.08	-.10	-.12	-.14	-.14	-.14	-.12	-.27
9	+.02	+.06	+.09	+.13	+.17	+.20	+.22	+.25
10	-.05	+.02	+.08	+.14	+.19	+.25	+.30	+.35
11	-.19	-.08	+.02	+.12	+.20	+.29	+.37	+.46
12	-.76	-.50	-.30	-.05	+.16	+.35	+.49	+.67

IV. Calculation of Temperature Difference

The application of the formulas set up in section A page 7, made it possible to pass from the pressure differ-

ences, or better, of the number $\frac{(p - p_0)}{(\rho_0 v_0^2/2)}$ to the temperature differences $\theta - t_0$. It was proved justifiable to employ, instead of the complete equation (12), the approximate equation (13), which may be expressed in the following form:

$$\theta - t_0 = v_0^2 \left[A + \frac{p_0 - p}{\rho_0 \frac{v_0^2}{2}} \left(A - \frac{1}{2c_p} \right) \right] \quad (14)$$

Here:

$$v_0 = 4,500 \text{ cm/s}$$

$$A = 4.2 \times 10^{-8} \text{ deg./}(\text{cm/s})^2$$

$$c_p = 10^7 \text{ ergs/gram deg.}$$

whence:

$$\theta - t_0 = 2025 \times 10^4 \left(4.2 \times 10^{-8} + \frac{p - p_0}{\rho_0 \frac{v_0^2}{2}} \times 0.8 \times 10^{-8} \right)$$

$$\theta - t_0 = 0.85^\circ + 0.16^\circ \frac{p - p_0}{\rho_0 \frac{v_0^2}{2}} \quad (15)$$

Then it is easy to pass from table II to table III, which contains the temperature differences $\theta - t_0$ obtained with equation (15).

TABLE III

Temp. difference tap	Incidence							
	-8.40°	-3.60°	-0.70°	+2.20°	+5°	+7.80°	+10.70°	+14.70°
1	0.38	0.65	0.85	0.97	1.01	1.00	0.94	0.82
2	.99	.96	.91	.85	.77	.66	.57	.43
3	.89	.83	.77	.70	.63	.54	.46	.35
4	.83	.78	.73	.67	.62	.55	.49	.42
5	.77	.73	.69	.64	.61	.57	.54	.51
6	.75	.74	.72	.69	.69	.66	.66	.69
7	.79	.78	.77	.77	.77	.76	.76	.80
8	.84	.84	.83	.83	.83	.83	.83	.81
9	.85	.86	.87	.87	.88	.88	.88	.89
10	.84	.85	.86	.87	.88	.89	.90	.91
11	.82	.84	.85	.87	.88	.90	.91	.92
12	.73	.77	.80	.84	.87	.91	.93	.96

V. Accuracy of the Preceding Data

1. First, it is attempted to ascertain the degree of accuracy which may be looked for in the experimental evaluation of $\theta - t_0$ (equation 14).

According to table I, the temperature difference $\theta - \theta_0$ between the relevant junction and junction R does not exceed, in absolute value, by $\frac{1}{2}^\circ$ the experimental conditions ($v_0 = 45$ m/s); it is repeatedly of the order of $1/10^\circ$. However, the experience we were able to gain in the many temperature measurements so far, does not permit us to guarantee this temperature difference any closer than around $1/20^\circ$.

The same absolute error figures in the term $\theta_0 - t_0$ and, for $v_0 = 45$ m/s, this term may be considered as ranging between 0.8° and 0.9° .

Lastly, $\theta - t_0$ may be affected by an absolute error of 0.1° . The measurements are therefore not very accurate, since the numerical values do not exceed 1° . We should have more accurate measurements at much higher speeds, and it might have been interesting, if this had been possible, to mount the model in a high-speed tunnel.

2. The result of computing $\theta - t_0$ by means of equation (15) is, as the experimental errors, such as affects

$$\frac{(p - p_0)}{(\rho_0 v_0^2 / 2)}, \quad \text{These errors amount, at the most, to 2 to 3}$$

percent. But allowance should also be made for the large systematic error which may follow the choice of the constant A . We took $A = 4.2 \times 10^{-8}$, which we had obtained precisely in the wind-tunnel tests for a wide range of speeds, but it may be that in actual tests the value of A drops to 4.0×10^{-8} ; in this particularly unfavorable case the formula for $\theta - t_0$ becomes:

$$\theta - t_0 = 0.805^\circ + 0.2025^\circ \frac{p - p_0}{\rho_0 \frac{v_0^2}{2}}$$

The discrepancy, as compared with equation (15), then exceeds 0.10° .

3. On the basis of these arguments as regards accuracy, which is the better formula for comparing the results - equation (14) (experimental), or equation (15) (theoretical)? The accidental errors being small in the figures of table III, the curves obtained are regular, starting with these figures, either by plotting the temperature readings (values of $\theta - t_0$ at various points of the wing for a given incidence), or by plotting $\theta - t_0$ against the incidence for a given point. Plotting the experimental points obtained by means of equation (14) on the preceding graphs, we either find the points located near the plotted curves - in which case the theory is verified within the indicated accuracy - or else distinctly greater discrepancies. In the latter case it may be attempted to ascertain whether a slightly different value of constant A would bring the curve closer to the experimental values.

VI. Temperature Readings

To plot the temperature readings (figs. 15 to 22), we take the normals to the 12 points of the wing to which the pressure or temperature corresponds, and trace on these normals lengths proportional to the figures contained in an

identical column of table III. The points thus obtained are then connected by solid line. Near the leading edge the trace of reading is not very accurate because of the great airfoil camber; in fact, in spite of the scarcity of test orifices in this zone, the points are fairly distant from each other. Moreover, a slight mistake in the position of test orifice no. 1, entails a great change in direction of the normal and consequently, in the position of the corresponding figurative point.

Then the values figuring in the corresponding column of table I are indicated on the same normals and the experimental points marked without plotting the curve.

Examination of the eight readings corresponding to the eight explored incidences allows the comparison of the theoretical and experimental results.

VII. Temperature Variation Curves against Incidence

The comparison is facilitated if the figures corresponding to one line of the tables are plotted on the same chart - that is, to say, for one temperature tap. The result is then the temperature variation versus incidence; the solid dash corresponds to the figures of table III (theory), and the dots to the figures in table I (test data). The result is: 12 charts (figs. 23 to 34) for 12 test taps.

VIII. Comparison of Theoretical and Experimental Results

On the whole, the experimental points approach the theoretical curves to within less than 0.10° . If the points corresponding to lead No. 8 are eliminated, for three measurements alone (four - twenty - four), the difference exceeds: (incidence -6.40° and junction No. 1; 0.11 , incidence -3.60° and junction No. 5; 0.13° , incidence $+10.70^\circ$ and junction No. 12; 0.11° , differences which are still compatible with what we could expect in the experiments.

The points are stationed - sometimes above, sometimes below the curves, which precludes the existence of large systematic departure. However, for lead No. 8 (fig. 30), the experimental points are distinctly above the curve; perhaps a structural defect (defective level of the junction, defect in the thermocouple circuit) was the cause of

tion, defect in the thermocouple circuit) was the cause of these differences.

It may be concluded from the foregoing results that formula (15) represents the experimental results obtained on the model and that the theory exposed in section A surely constitutes a first acceptable approximation.

D. RESULTS OF TESTS WITH A WING

I. Test Conditions

The measurements were made November 17, and 18, 1936, in the large wind tunnel at Chalais-Meudon. Here, the wing incidence adjustment required the stopping of the tunnel. Again it was necessary to make eight series of measurements corresponding to different incidences (-6.1° , -3.1° , 0° , 3.1° , 6.1° , 9.1° , 12.2° , 16.4°). These incidences are those of the tangent to the lower camber of the Göttingen airfoil section No. 387; they were corrected for wall effect. The air speed ranged around 38 m/s. Only one test series, that of incidence 6.1° , was repeated after a one-day interval.

II. Temperature Recording Table

Table IV gives, for each incidence, the value of temperature difference $\theta - t_0$ at the different junctions marked from 1 to 13 (θ , junction temperature; t_0 , temperature of air in infinite stream). Junction No. 1 corresponds to that located at the leading edge; those from 2 to 8, to junctions on the top camber, counting from nose to tail; Nos. 9 to 13, to the junctions on the bottom camber, counting from tail toward leading edge. Figure 12 illustrates both the location and numbers of the junctions.

Again, the rough result of the measurement is the difference between temperature θ of the junction and temperature θ_0 of the reference junction r located a little upstream from the wing. We pass from $\theta - \theta_0$ to $\theta - t_0$ by adding the term $\theta_0 - t_0$ which, for 38 m/s speed, is about 0.60° (formula $\theta_0 - t_0 = 4.2 \times 10^{-8} v_0^2$ is used consistently). These are the differences $\theta - t_0$ given in table IV.

TABLE IV

Test ori- fices	Incidence							
	-6.10°	-3.10°	+0°	+3.10°	+6.10°	+9.10°	+12.20°	+16.40°
1	0.56°	0.62°	0.71°	0.73°	0.60°	0.71°	0.56°	0.39°
2	.73°	.68°	.67°	.60°	.52°	.35°	.24°	.16°
3	.58°	.52°	.49°	.44°	.37°	.26°	.18°	.10°
4	.56°	.50°	.45°	.32°	.38°	.22°	.21°	.16°
5	.43°	.46°	.42°	.37°	.44°	.32°	.31°	.34°
6	.55°	.52°	.47°	.54°	.49°	.50°	.44°	.51°
7	.58°	.59°	.57°	.60°	.56°	.57°	.58°	.54°
8	.62°	.66°	.69°	.65°	.63°	.64°	.64°	.56°
9	.61°	.62°	.66°	.65°	.64°	.66°	.66°	.66°
10	.59°	.62°	.61°	.65°	.62°	.66°	.67°	.67°
11	.55°	.58°	.61°	.64°	.62°	.65°	.67°	.68°
12	.48°	.58°	.56°	.61°	.62°	.69°	.70°	.72°
13	.31°	.40°	.48°	.60°	.63°	.70°	.68°	.72°

III. Pressure Recording Table

Toward the middle of a test series a multiple manometer connected to the different pressure taps is photographed. We thus obtain

TABLE V

Test ori- fices	Incidence							
	-6.10°	-3.10°	0°	+3.10°	+6.10°	+9.10°	+12.20°	+16.40°
1	0.30	0.66	1.00	1.00	0.76	0.31	-0.48	-1.10
2	.92	.79	.42	-.21	-.71	-1.38	-2.09	-2.47
3	.13	-.11	-.48	-.98	-1.41	-1.87	-2.31	-2.37
4	-.37	-.53	-.86	-1.22	-1.50	-1.76	-2.00	-1.85
5	-.55	-.67	-.86	-1.04	-1.18	-1.28	-1.33	-.89
6	-.40	-.44	-.54	-.58	-.62	-.64	-.51	-.55
7	-.21	-.23	-.27	-.27	-.27	-.24	-.23	-.54
8	.07	.07	.07	.09	.07	.04	-.13	-.47
9	.10	.11	.14	.18	.19	.20	.19	.11
10	.00	.02	.09	.15	.20	.25	.27	.27
11	-.18	-.10	.01	.13	.22	.30	.36	.41
12	-.59	-.42	-.14	.14	.31	.46	.62	.70
13	-1.52	-1.10	-.48	.05	.38	.67	.87	.97

which contains the differences between the pressure p at the various pressure taps and the static pressure p_0 in the undisturbed stream. A second manometric tube connected to a pitot tube gives the value of $\rho_0 v_0^2/2$ at the same instant. These values are given nondimensionally $(p - p_0)/(\rho_0 v_0^2/2)$ in table V.

IV. Calculation of Temperature Differences

As before, the change from $\frac{(p - p_0)}{(\rho_0 v_0^2/2)}$ to temperature differences $\theta - t_0$ is effected by means of formula:

$$\theta - t_0 = v_0^2 \left[A + \frac{p_0 - p}{\rho_0 v_0^2/2} \left(A - \frac{1}{2c_p} \right) \right]$$

and on the basis of $A = 4.2 \times 10^{-8} \text{ deg.}/(\text{cm/s})^2$ and $c_p = 10^7$ ergs/gram deg., but, here, $v_0 = 3,800 \text{ cm/s}$, hence:

$$\theta - t_0 = 0.60^\circ + 0.12^\circ \frac{p_0 - p}{\rho_0 v_0^2/2} \quad (16)$$

The temperature differences $\theta - t_0$ computed by means of equation (16), are tabulated in table VI.

TABLE VI

Test orifices	Incidence							
	-6.10°	-3.10°	0°	3.10°	6.10°	9.10°	12.20°	16.40°
1	0.63°	0.68°	0.72°	0.72°	0.69°	0.64°	0.54°	0.47°
2	.71°	.69°	.65°	.57°	.51°	.43°	.35°	.30°
3	.61°	.59°	.54°	.48°	.43°	.38°	.32°	.32°
4	.56°	.54°	.50°	.45°	.42°	.39°	.36°	.38°
5	.53°	.52°	.50°	.47°	.46°	.45°	.44°	.49°
6	.55°	.55°	.53°	.53°	.53°	.52°	.54°	.53°
7	.58°	.57°	.57°	.57°	.58°	.57°	.57°	.53°
8	.61°	.61°	.61°	.61°	.61°	.60°	.58°	.54°
9	.61°	.61°	.62°	.62°	.62°	.62°	.62°	.61°
10	.60°	.60°	.61°	.62°	.62°	.62°	.63°	.63°
11	.58°	.59°	.60°	.62°	.63°	.64°	.64°	.64°
12	.53°	.55°	.58°	.62°	.64°	.65°	.67°	.67°
13	.42°	.48°	.54°	.61°	.65°	.68°	.70°	.72°

V. Accuracy of Results

As in the model tests, the direct measurements of $\theta - t_0$ are subject to an error of 0.1° . When the speed is slower the accuracy certainly is not as good as in the model tests.

Then, too, since the measurements were not, as a rule, repeated, there is no information as to the fidelity of the measurements. Five series of tests were made on November 17 (incidences -6.1° , -3.1° , 0° , 3.1° , 6.1° ; for the next day (incidences 6.1° , 9.1° , 12.2° , 16.4°); those for 6.1° were repeated two days later. The results were as follows:

Test orifice	1	2	3	4	5	6	7
Nov. 17	0.66°	0.52°	0.37°	0.38°	0.44°	0.49°	0.56°
Nov. 18	$.68^\circ$	$.46^\circ$	$.30^\circ$	$.28^\circ$	$.34^\circ$	$.48^\circ$	$.58^\circ$
Test orifice	8	9	10	11	12	13	
Nov. 17	0.63°	0.64°	0.62°	0.62°	0.62°	0.63°	
Nov. 18	$.64^\circ$	$.63^\circ$	$.63^\circ$	$.64^\circ$	$.62^\circ$	$.60^\circ$	

The figures at times are distinctly different; besides, even the pressure measurements themselves manifest notable discrepancies, as seen from the following:

Test orifices	1	2	3	4	5	6	7
Nov. 17	0.76	-0.71	-1.41	-1.50	-1.18	-0.62	-0.27
Nov. 18	.65	-.93	-1.55	-1.57	-1.21	-.62	-.25
Test orifices	8	9	10	11	12	13	
Nov. 17	0.07	0.19	0.20	0.22	0.31	0.38	
Nov. 18	.05	.19	.20	.23	.34	.48	

In the face of such discrepancies, which are much greater than in the model test, the interest in the wing measurement drops considerably. To compare the theoretical (table VI) with the experimental results (table IV), we limit ourselves to plotting the temperature readings.

VI. Temperature Readings

The procedure is the same as for the model; the curves present the theoretical $\theta - t_0$, and the points, the corresponding experimental values. The eight readings (figs. 35 to 42) relate to the eight explored incidences. The graph for 6.1° was plotted by means of the values observed on November 17.

VII. COMPARISON

The tests made on November 17 must be separated from those made on November 18.

As to the five test series of November 17, it may be said that the experimental check with the theoretical results. The discrepancies do not exceed 10° except for two points over 65 and they correspond to two consecutive measurements (test orifices 4 and 5, incidence 3.1°).

Contrariwise, the three test series of November 18, disclosed large and systematic discrepancies at orifices 2, 3, 4, and 5 which, at great positive incidences, correspond to the depression zone over the top surface. One plausible explanation for this strange behavior is that the imputed observations are precisely those made at the beginning of the tests. The tests may have been made rather fast on November 18 - the steady regime not quite reached - so that the junctions had not as yet attained their steady temperature at the time the measurement was taken. In fact, as already stated in V (p. 27), the November 18 measurements do not seem to confirm those of November 17, and this holds for both the temperature and the pressures. I do not think that much importance attaches to the discrepancies of November 18.

In conclusion, and bearing in mind - above all - the fidelity of the results observed on the model, it may be said that the simple theory explained in section A, is

practical enough for evaluating the temperatures at different points of a single wing and deducing the distribution of the pressures and temperatures. In particular, in the case of the wing investigated here, we take as results to be examined, those which express the theoretical curves plotted above (figs. 35 to 42).

D. APPLICATION OF TEMPERATURE MEASUREMENTS ON A WING

I. Wing Warmer Than Air

The plotted temperature readings prove that in steady regime the different zones of a wing are all warmer than the air in which the wing moves.

1. At points of the wing where positive pressure prevails, the heat effects due to friction and those due to compression, all contribute separately to the heating of the wing. The positive pressure, incidentally, is maximum in the dead point, for which we have the equality $p = p_0 + \rho_0 v_0^2/2$; for this point $(p - p_0)/(\rho_0 v_0^2/2)$ is maximum and equal to 1. Consequently, according to equation (13), the heating is also maximum and equal to

$$\theta_m - t_0 = \frac{v_0^2}{2c_p}$$

which, with $c_p = 10^7$ ergs/gram deg., gives:

$$\theta_m - t_0 = 5 \times 10^{-8} v_0^2$$

Hence, at points of the wing where it is maximum, the heating reaches 5° for a speed of 360 k.p.h. (223 n.p.h.).

2. At the points on the wing where depression prevails, the thermic effects due to friction and those due to depression are restrained, but the usual result is a heating because the thermic effect due to friction exceeds, as a rule, that due to depression. What is necessary, in fact, in order that a point of the wing shall have the temperature of the undisturbed flow? It is necessary that the value of $(p - p_0)/(\rho_0 v_0^2/2)$ is such that the difference $\theta - t_0$ becomes zero:

$$\theta - t_0 = v_0^2 \left[A + \frac{p - p_0}{\rho_0 v_0^2 / 2} \left(\frac{1}{2c_p} - A \right) \right] = 0$$

which gives:

$$\frac{p - p_0}{\rho_0 v_0^2 / 2} = \frac{A}{A - \frac{1}{2} c_p}$$

With $A = 4.2 \times 10^{-8}$ deg./ $(\text{cm/s})^2$

$$\frac{p - p_0}{\rho_0 v_0^2 / 2} = - \frac{4.2}{0.8} \sim 5$$

This value is not encountered in ordinary flying conditions.

II. Change of Temperature with the Speed

The temperature at the various points increases proportionally to the square of the speed if the law of pressure distribution - that is, to say, the local values of $(p - p_0)/(\rho_0 v_0^2 / 2)$ - does not vary with the Reynolds Number (equation 13).

In passing from the model to the wing tests, the dimensions are altered in the ratio of 5 to 1.1, and the speed in the ratio of 38 to 45, so that the Reynolds Number is approximately multiplied by 4. Are the values of $(p - p_0)/(\rho_0 v_0^2 / 2)$ noticeably changed? The test taps, numbers 3 and 12 on the wing (one on top, the other on bottom surface) are plainly coincident with those on the model. Plotting for taps 3 and 12, the curves giving $(p - p_0)/\rho_0 v_0^2 / 2$ against the incidence (figs. 43 and 44) it is observed that, even when disregarding that which occurs at high incidence where the discrepancies are very pronounced, the differences between the curves for the wings and those of the model are largely above 10 percent. These differences can even become greater if one passes from the case of the wing at 38 m/s to the practical case of a wing at 76 m/s (270 k.p.h.). Hence the statement that this local heating is proportional to the square of the speed, is an approximation.

III. Temperature Distribution

1. Toward the tail the temperature always approaches the value

$$\theta = t_0 + 4.2 \times 10^{-8} v^2$$

It is little affected by the incidence of the wing.

2. But, near the leading edge the results vary with the incidence. For negative incidence - that is, toward the top camber - the temperature is higher, while on the bottom camber a depression zone defines the cooler region. At positive incidence the depression passes to the top camber; it is there that elevation of the temperature will be least. The bottom camber, on the contrary, is the hot zone.

Some figures are given for an airplane at 300 k.p.h. (obtained on the premise of local heating proportional to the square of the speed). At -6° incidence, the excess $\theta - t_0$ of local temperature θ over the air temperature t_0 is in proximity of the leading edge - 1.5° toward the bottom camber, while reaching 3.5° toward the top camber. At positive incidence the excess $\theta - t_0$ is 3.5° at the leading edge but may drop over the top camber as much as 1.5° for 15° incidence.

IV. Effect of the Nature of the Wing

It is to be remembered that the experiments were made on a single wing and that no allowance was made for the thermal conductivity in the wing mass. Incidentally, the heat exchanges of a wing with the atmosphere (by forced convection) are of greater importance than those which may be observed in the material (by conduction); the thickness of the metal of which the wing is made is always small. The substitution of a metal wing for an isolated wing evidently acts in the sense of making the temperatures uniform, tied to the existence of a heat flow from the warmer toward the cooler points, but the results will nevertheless not be substantially different.

Translation by J. Vanier,
National Advisory Committee
for Aeronautics.

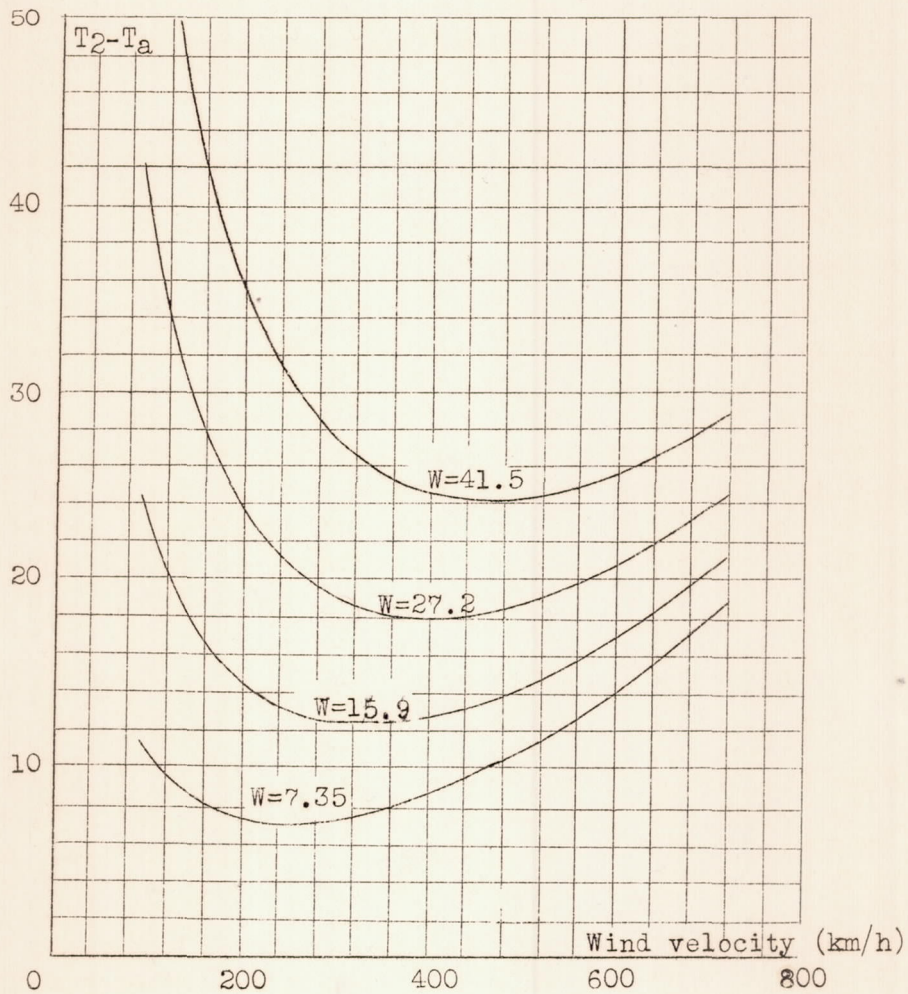


Figure 1.- Curves of constant heating giving excess temperature of a Balin antenna at altitude 0° .

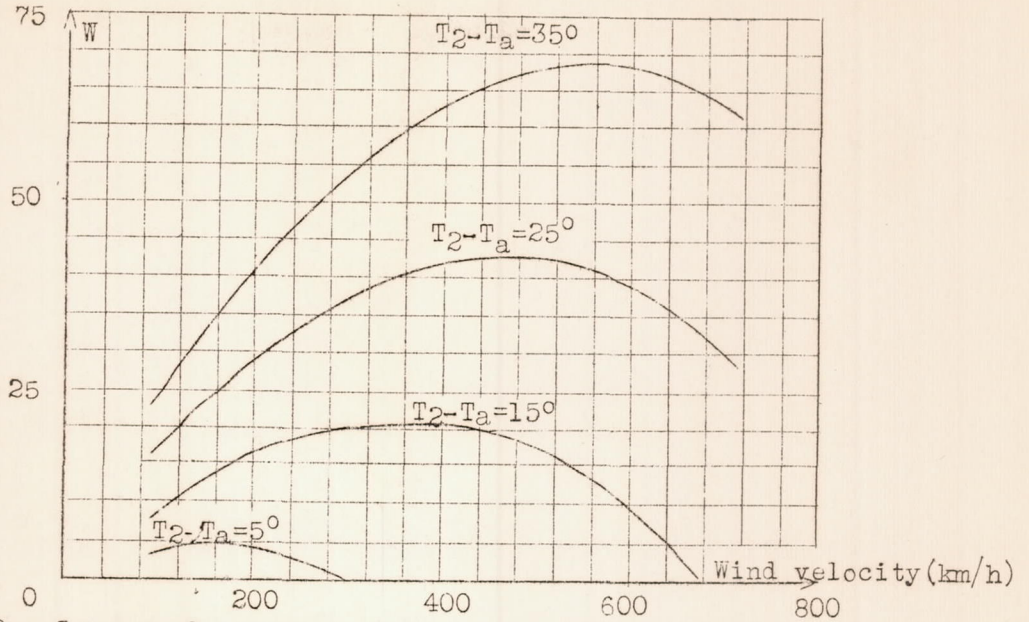


Figure 2.- Curves of constant temperature difference giving the heat of a Badin antenna at altitude 0°.

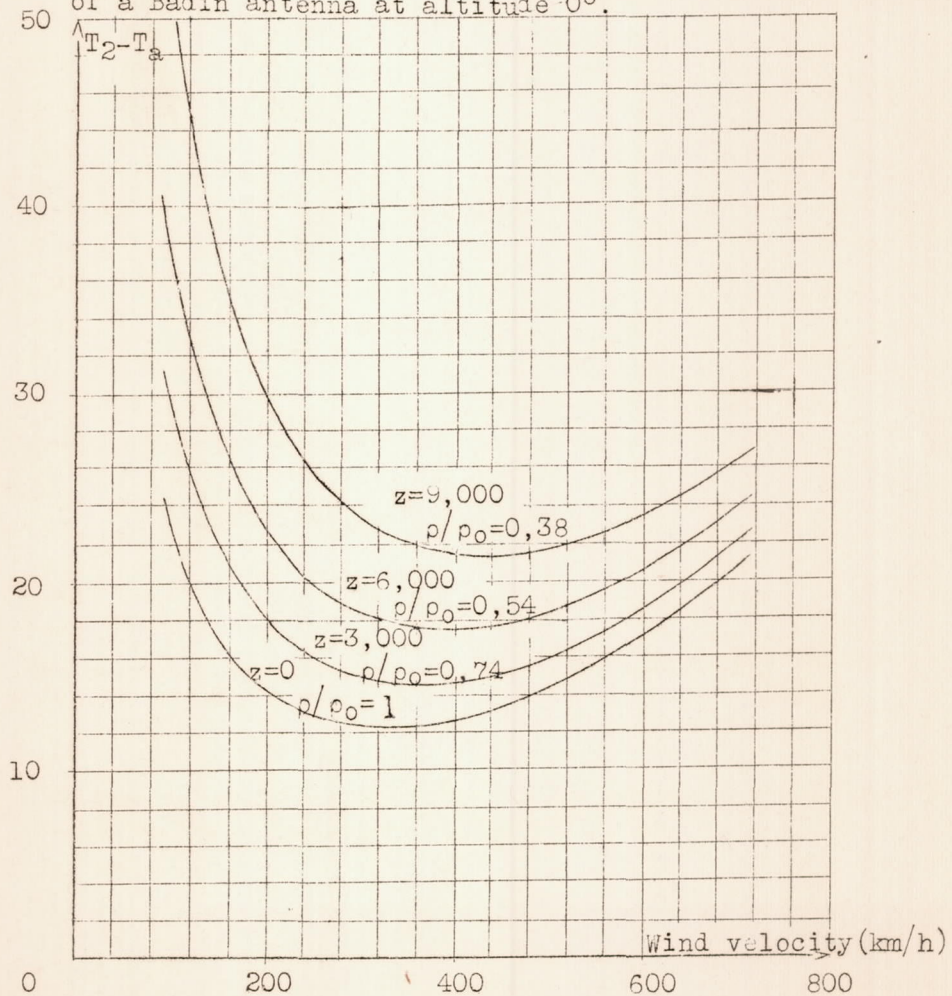


Figure 3.- Effect of altitude on temperature difference of a Badin antenna at 15.9 watt power input.

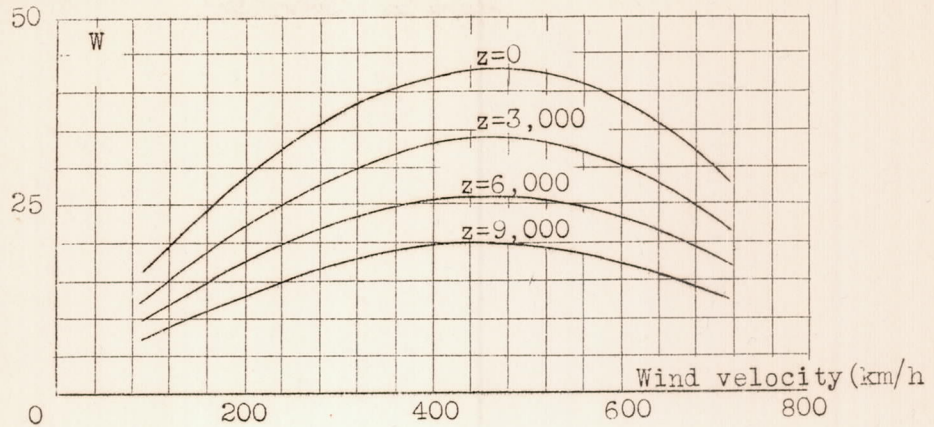


Figure 4.- Effect of altitude on the power dissipation of the Badin anemometer having a temperature 25° higher than the atmosphere.

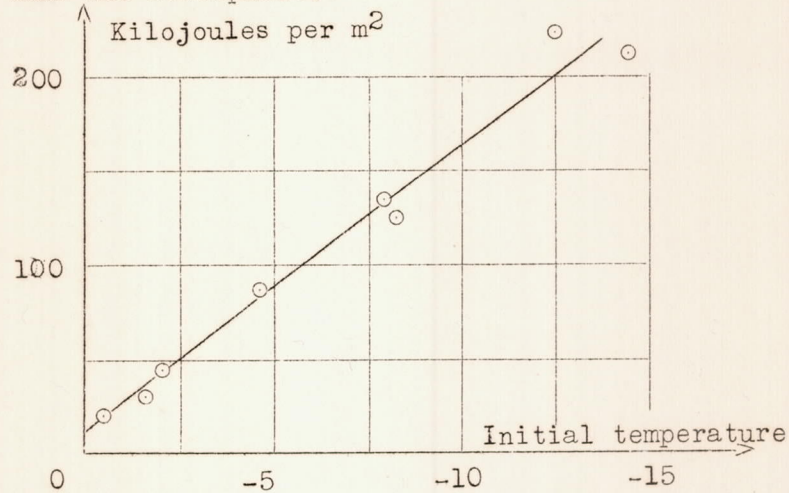


Figure 5.- Curve of energy required for de-icing in relation to initial temperature.

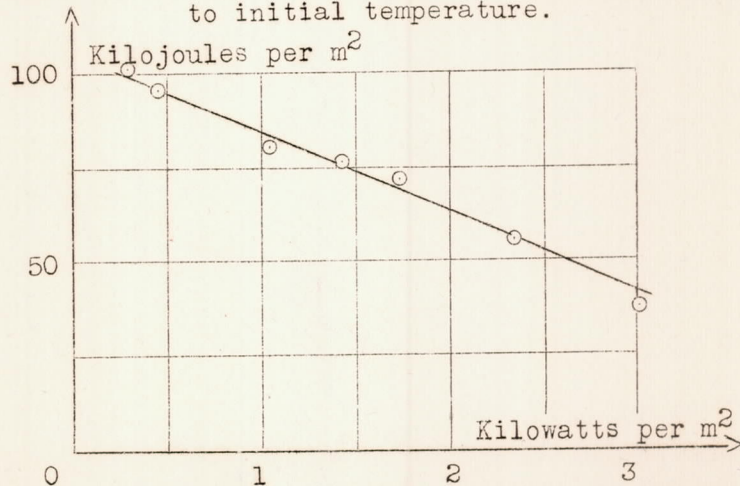


Figure 6.- Curve of energy required for de-icing plotted against horse power. (initial constant temperature)

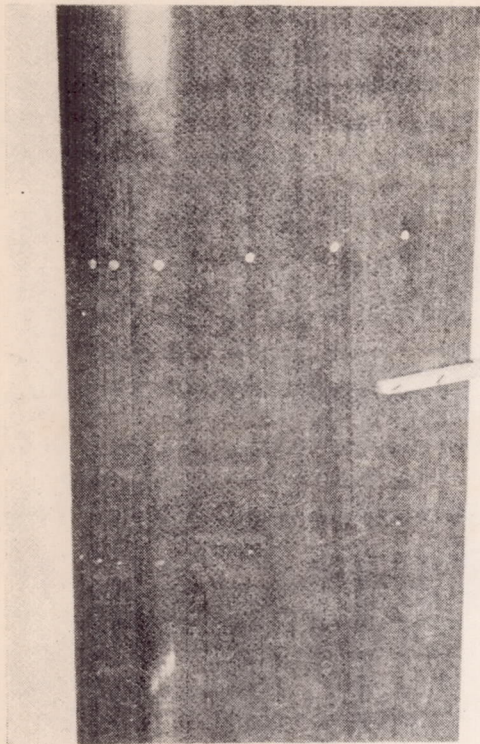


Figure 7.- Pressure and temperature taps on model.

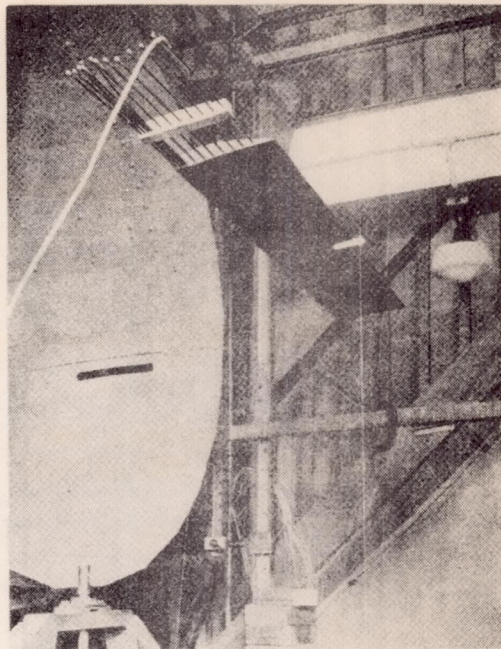


Figure 10.- Model mounted in tunnel.

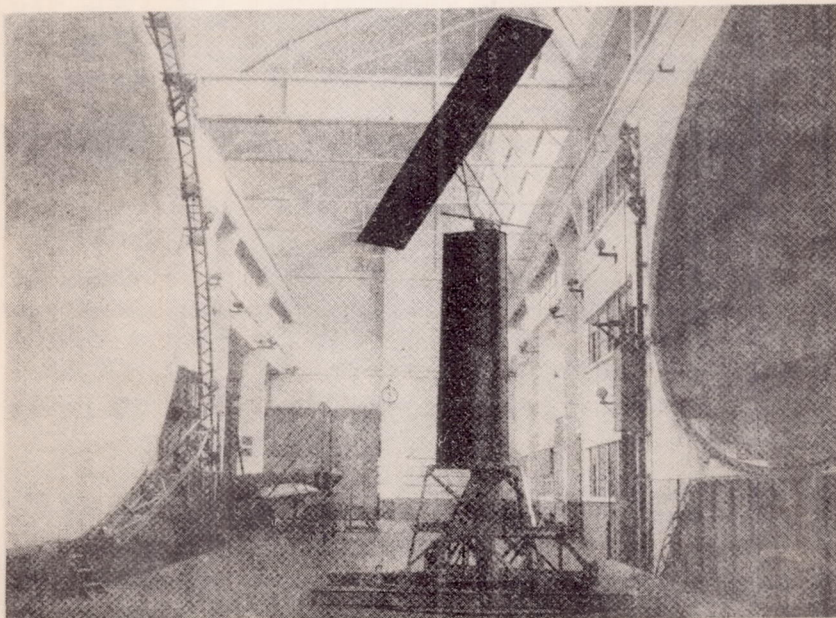


Figure 14.- Wing mounted for test.

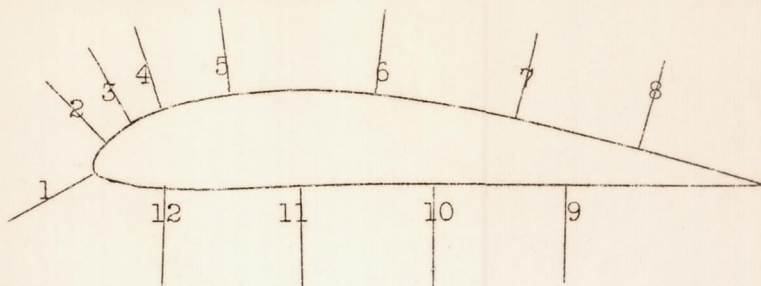


Figure 8.- Pressure and temperature stations on the model.

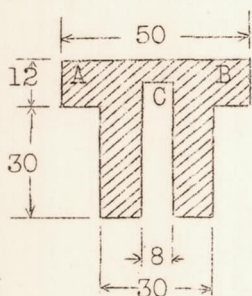


Figure 9.- Temperature tap fitting.

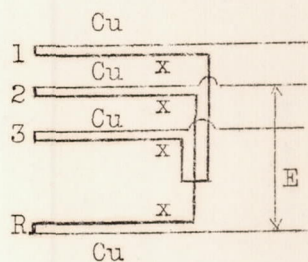


Figure 11.- Circuit of thermocouples(3).

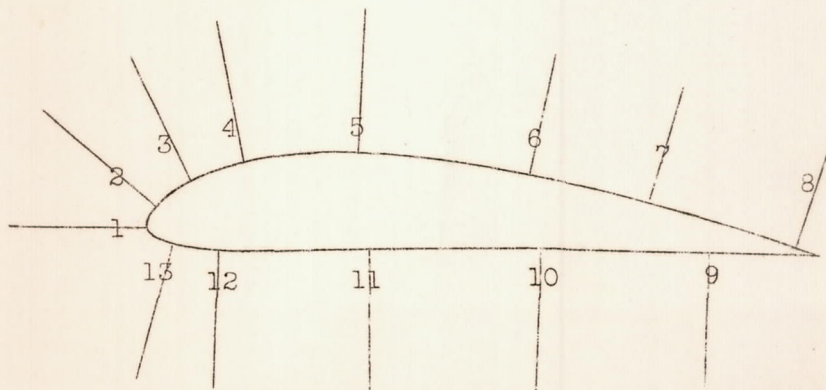


Figure 12.- Pressure and temperature stations on wing.

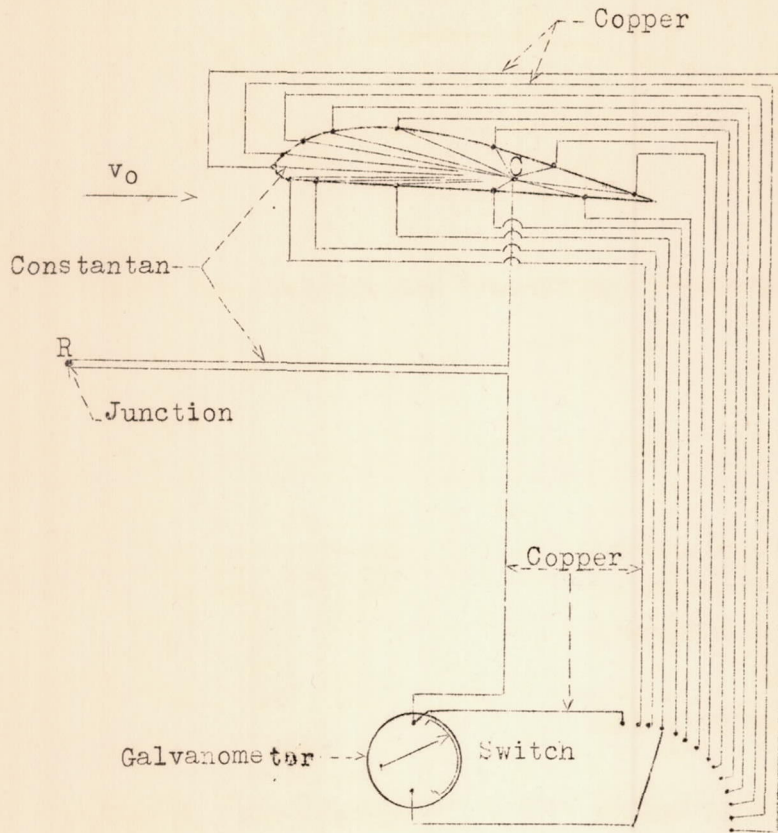


Figure 13.- Mounting of thermocouples in the wing.

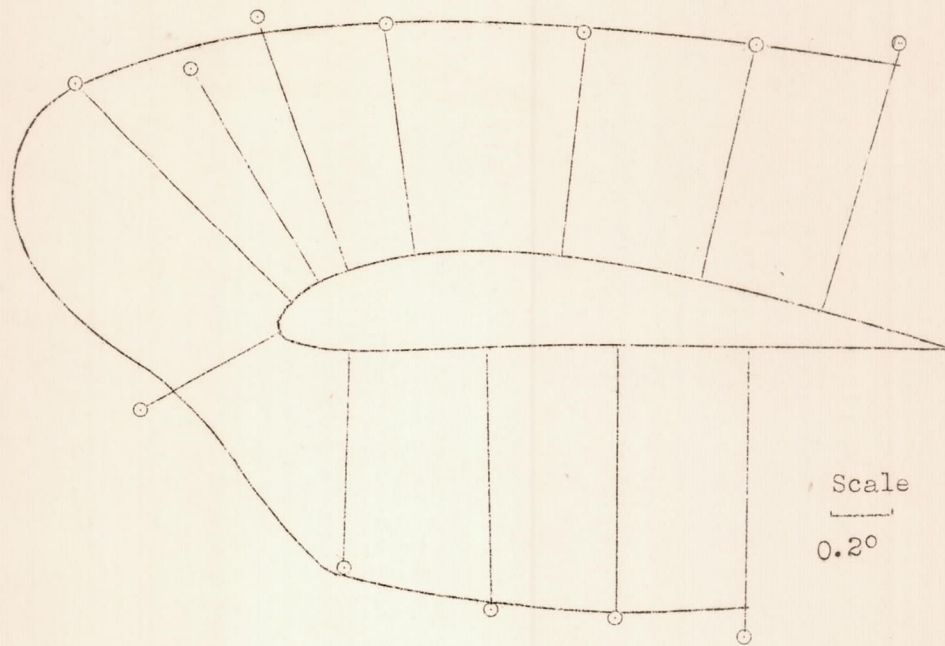


Figure 15.- Temperature record at -6.40° incidence(model)..

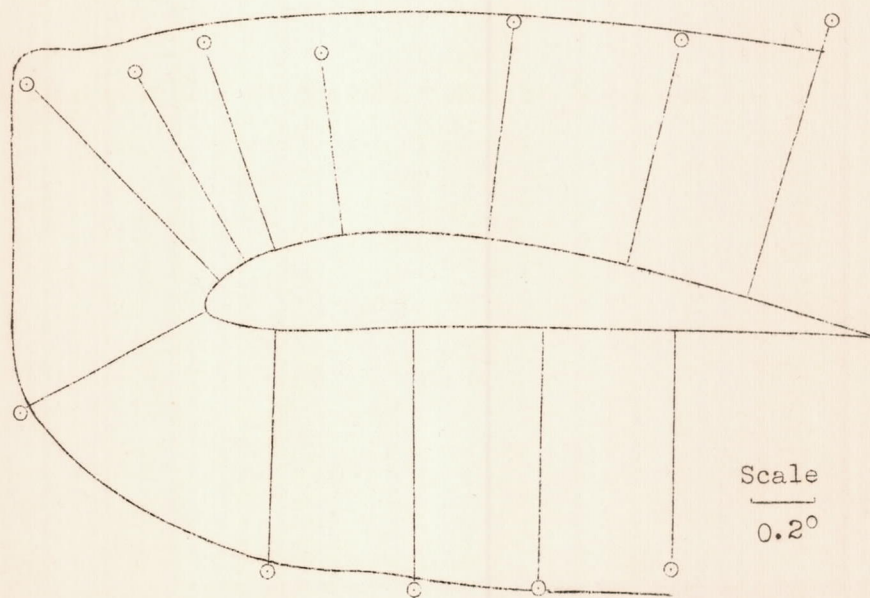


Figure 16.- Temperature record at -3.60° incidence(model)

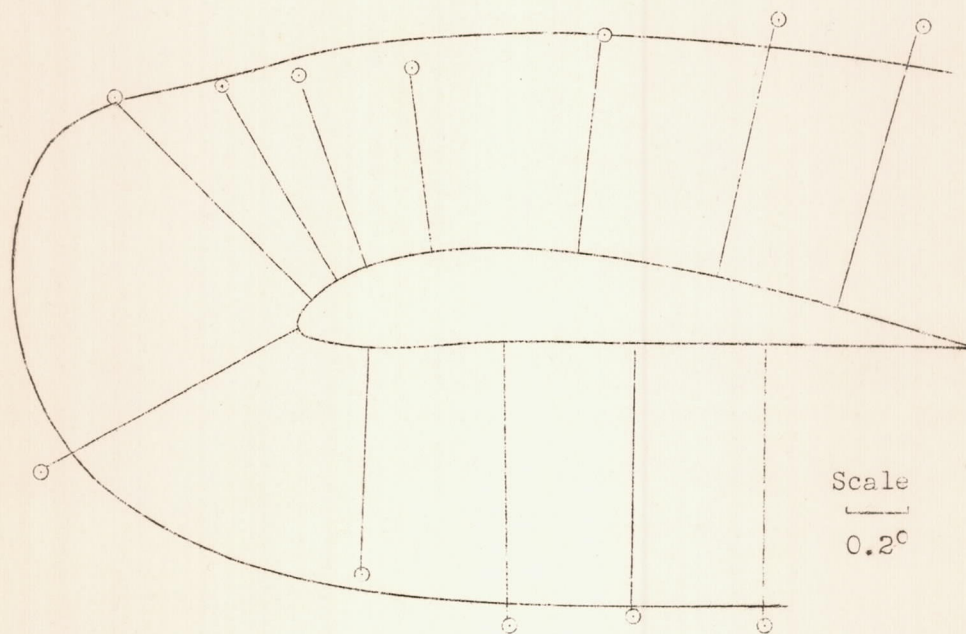


Figure 17.- Temperature record at $.7^\circ$ incidence(model)

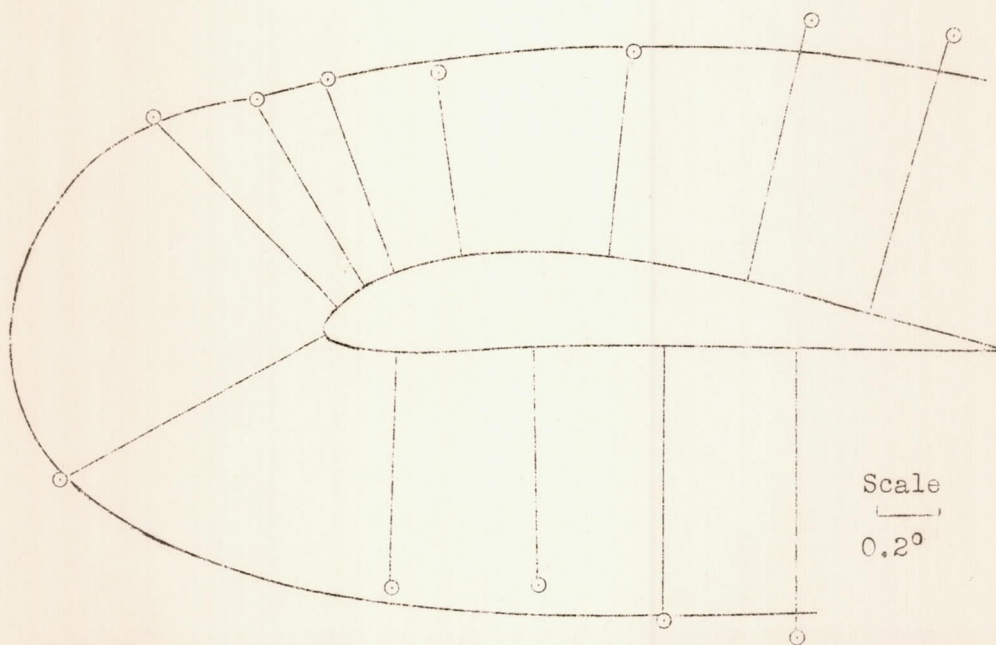


Figure 18.- Temperature record at 2.20° incidence(model).

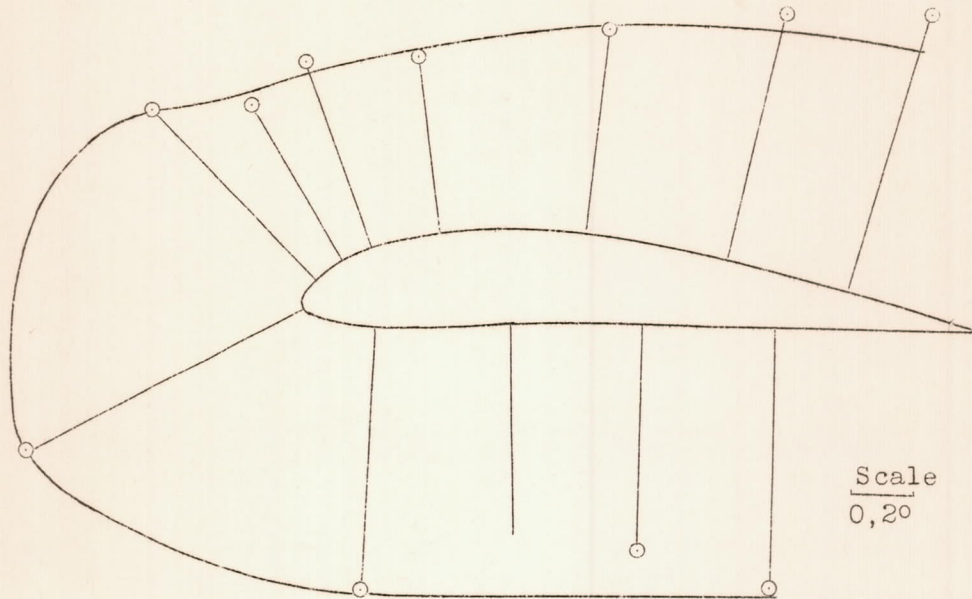


Figure 19.- Temperature record at 5° incidence. (model)

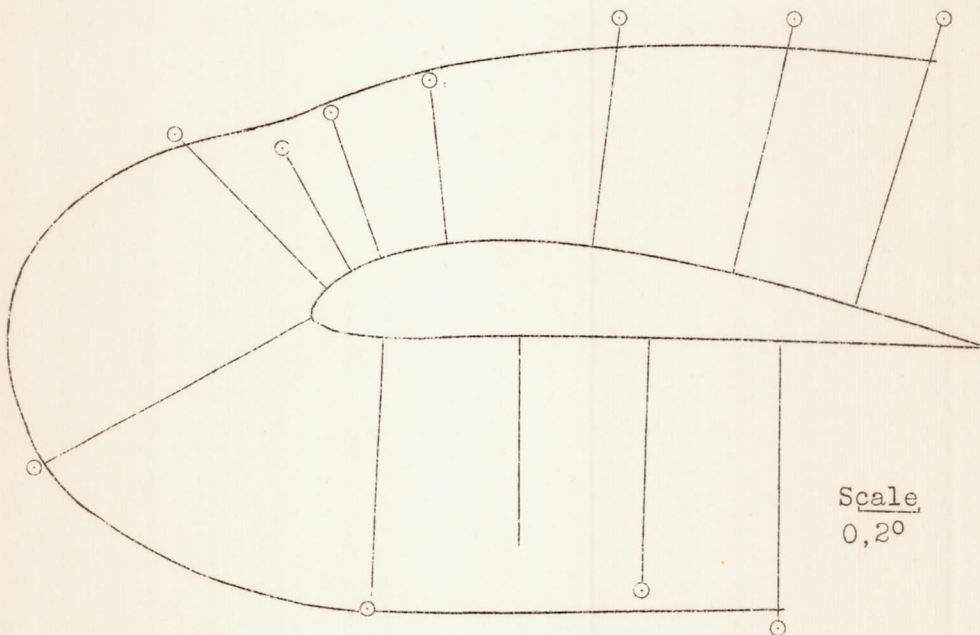


Figure 20.- Temperature record at 7,80° incidence. (model)

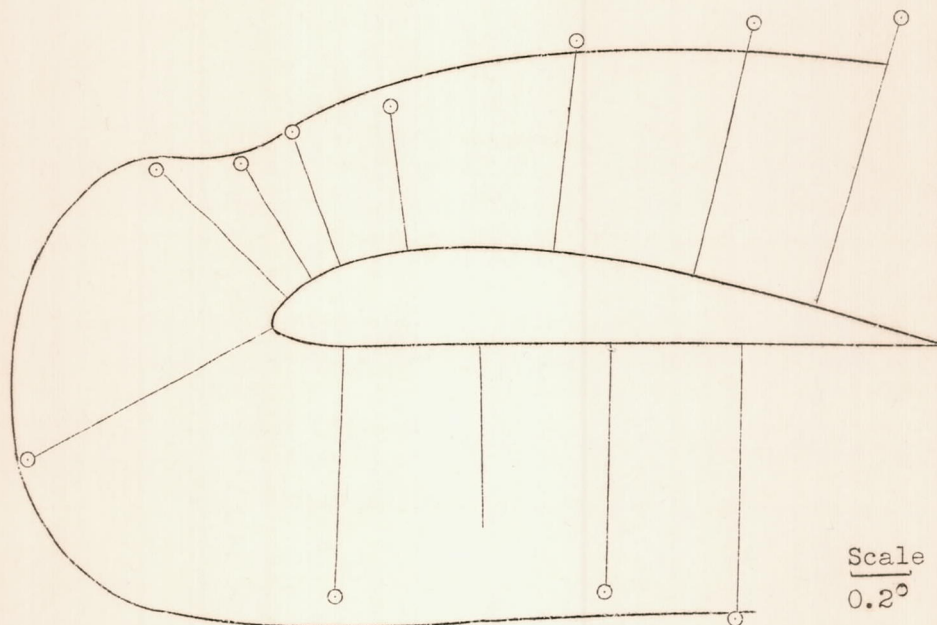


Figure 21.-- Temperature record at 10.7° incidence(model)

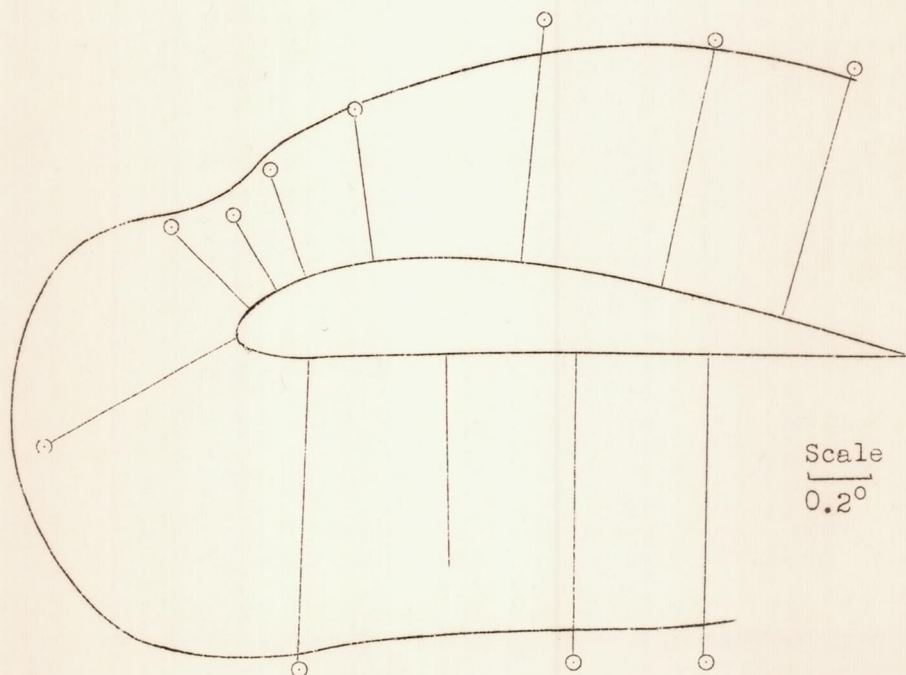


Figure 22.-- Temperature record at 14.7° incidence(model).

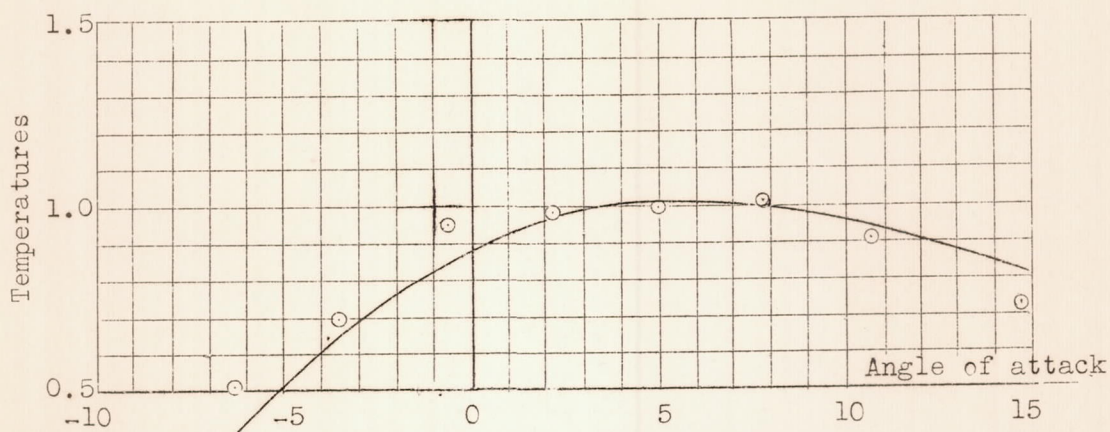


Figure 23.- Temperature curves of tap 1 plotted against the angle of attack(model)

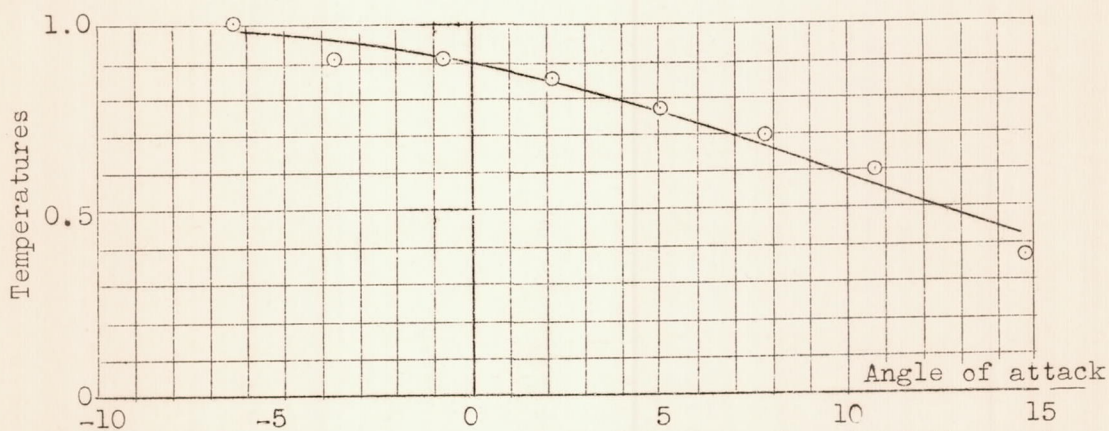


Figure 24.- Temperature curves of tap 2 plotted against the angle of attack(model)

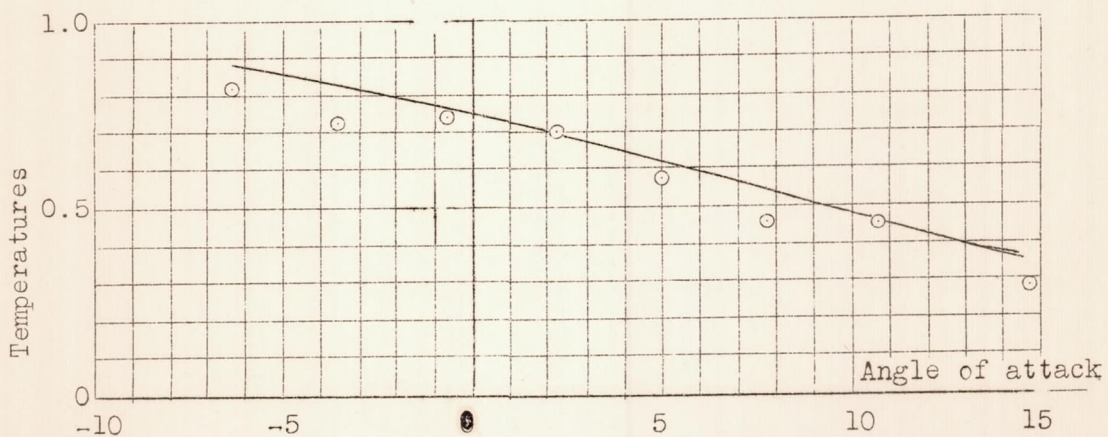


Figure 25.- Temperature curves of tap 3 plotted against the angle of attack(model)

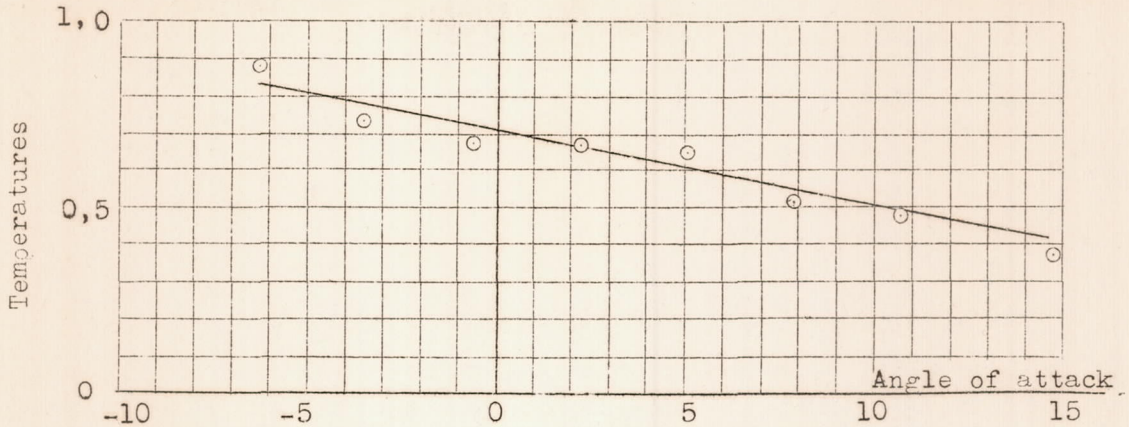


Figure 26.- Temperature curves of tap 4 plotted against angle of attack. (model)

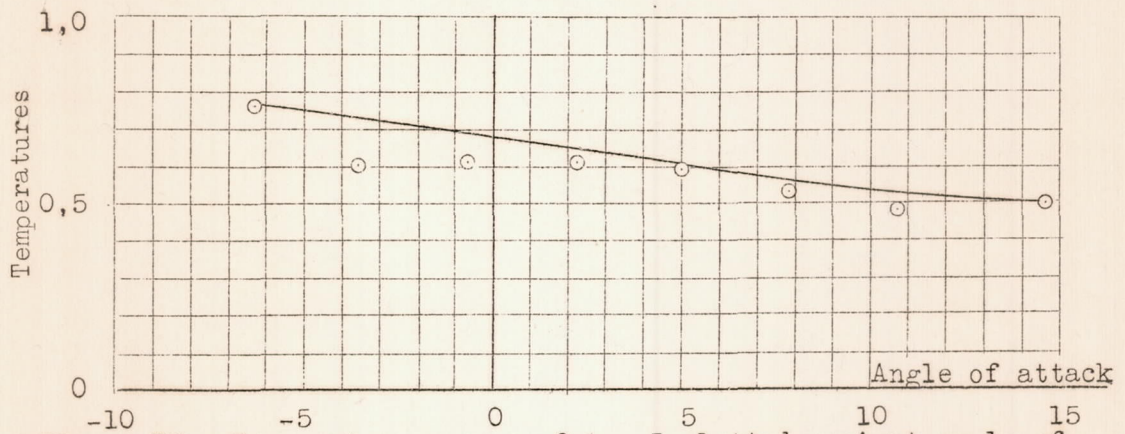


Figure 27.- Temperature curves of tap 5 plotted against angle of attack. (model)

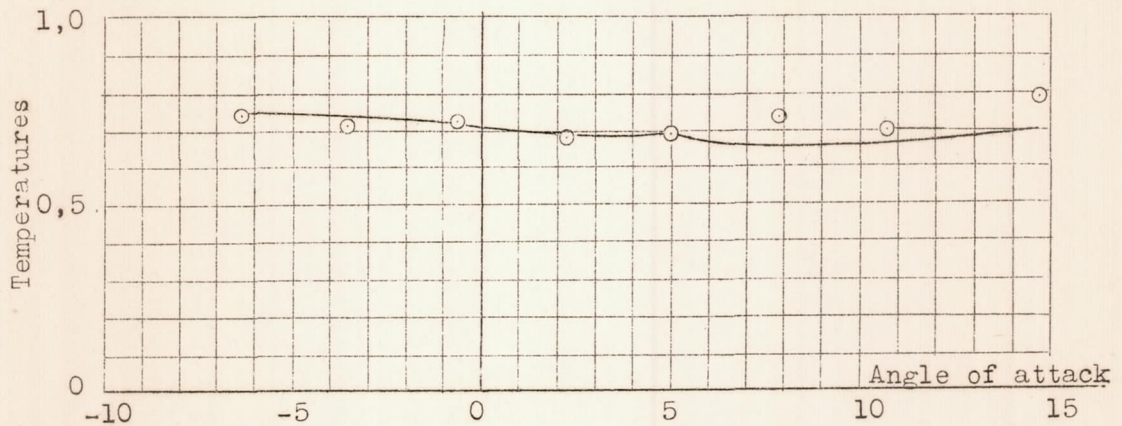


Figure 28.- Temperature curves of tap 6 plotted against angle of attack. (model)

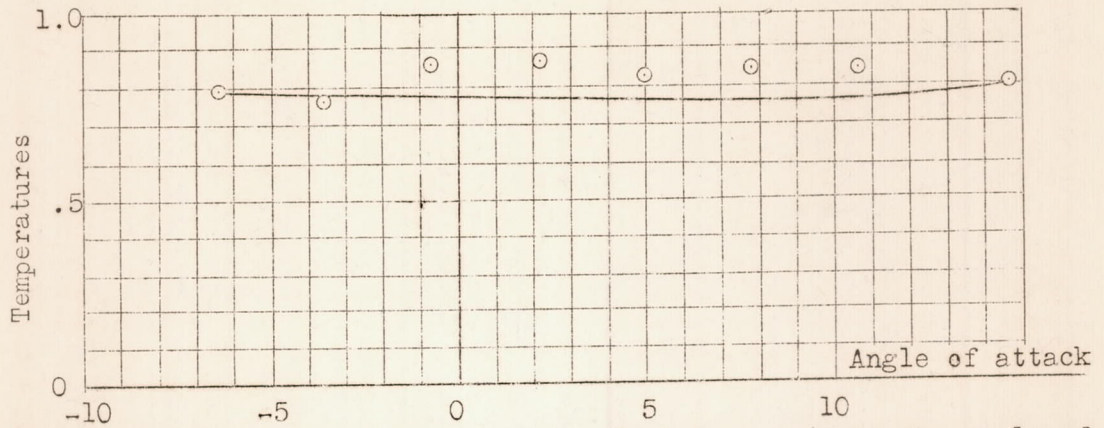


Figure 29.- Temperature curves of tap 7 plotted against the angle of attack(model).

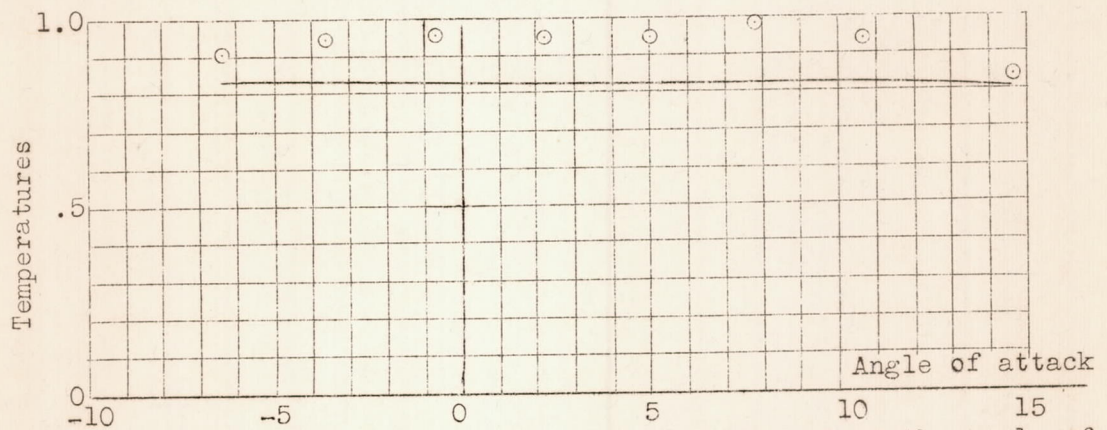


Figure 30.- Temperature curves of tap 8 plotted against the angle of attack(model).

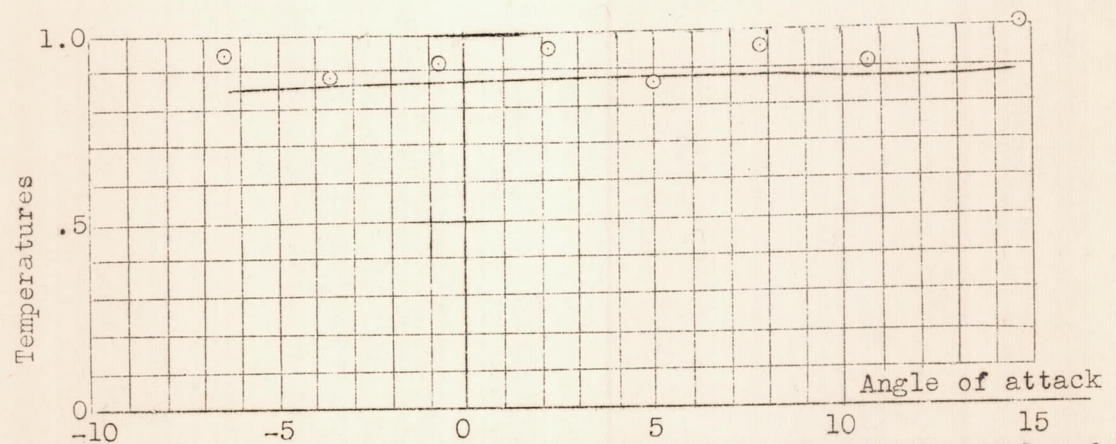


Figure 31.- Temperature curves of tap 9 plotted against the angle of attack(model).

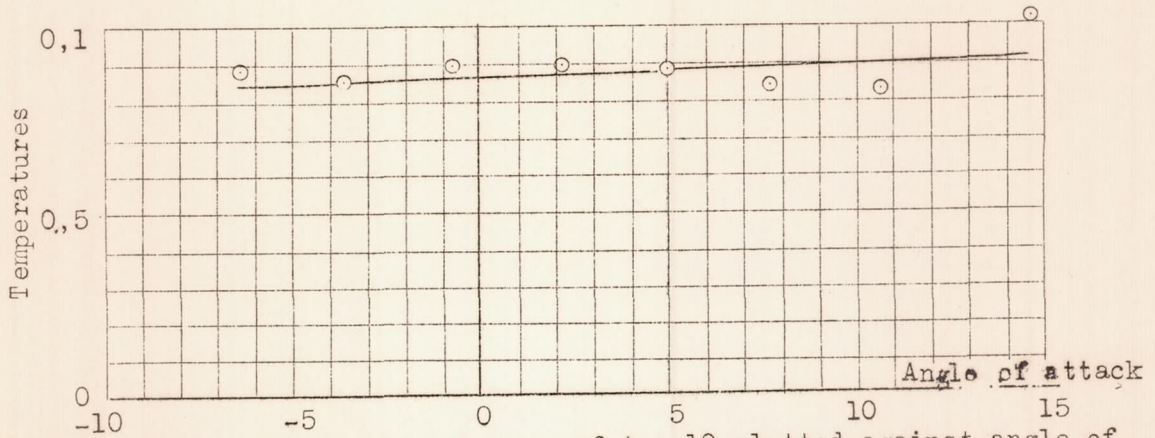


Figure 32.- Temperature curves of tap 10 plotted against angle of attack. (model)

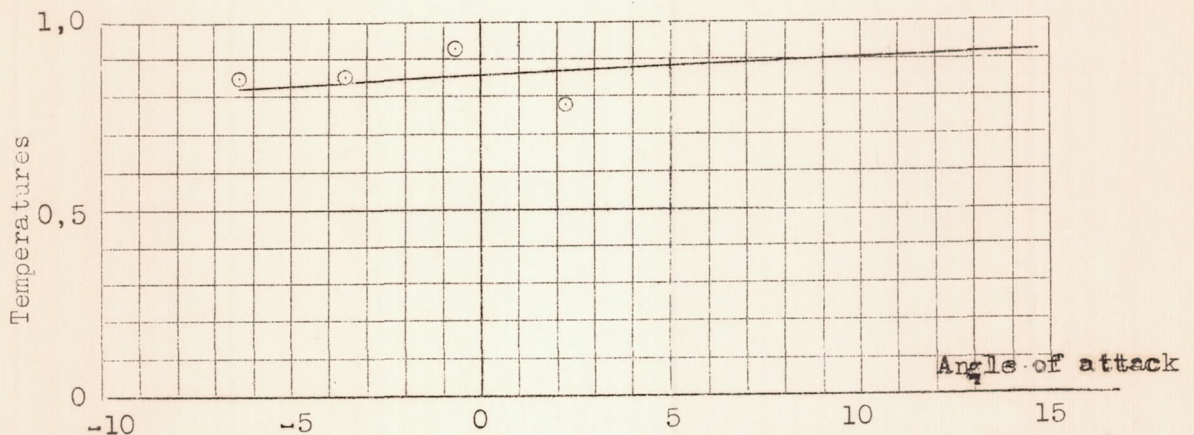


Figure 33.- Temperature curves of tap 11 plotted against angle of attack. (model)

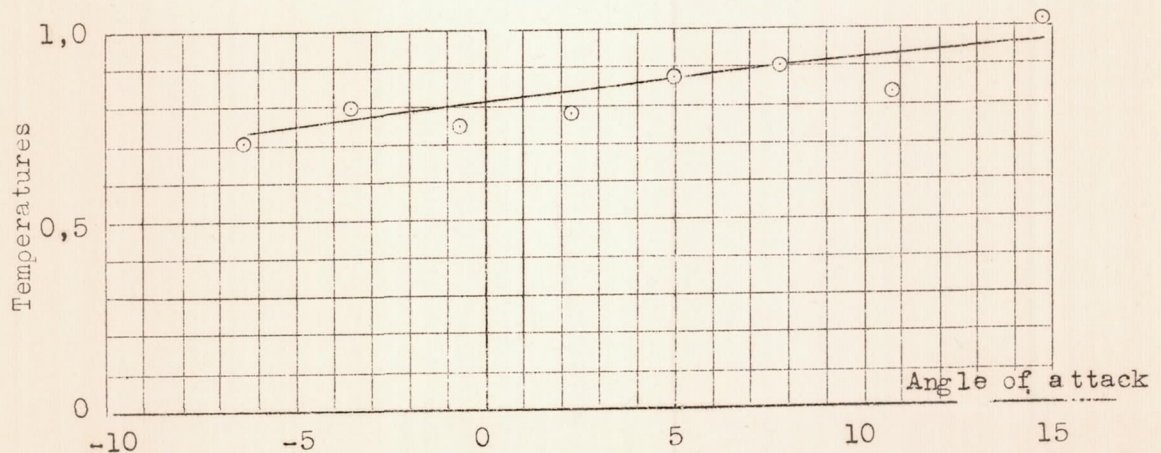


Figure 34.- Temperature curves of tap 12 plotted against angle of attack. (model)

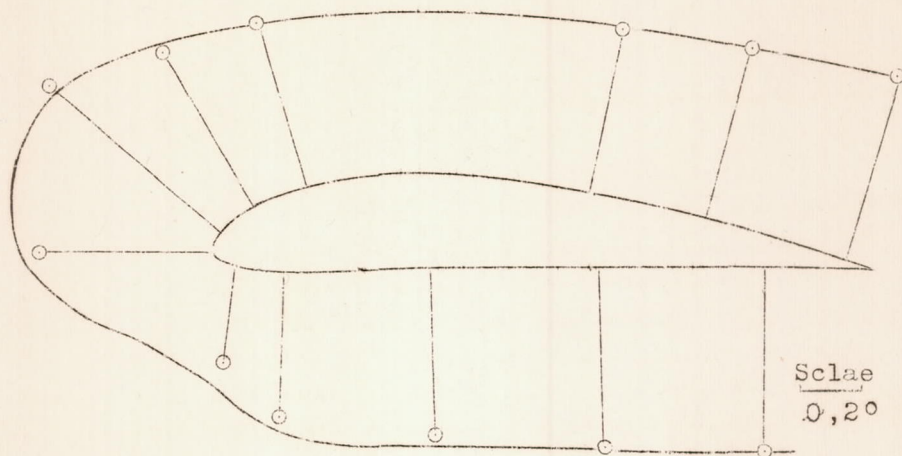


Figure 35.- Temperature record at $-6,1^\circ$ incidence. (wing)

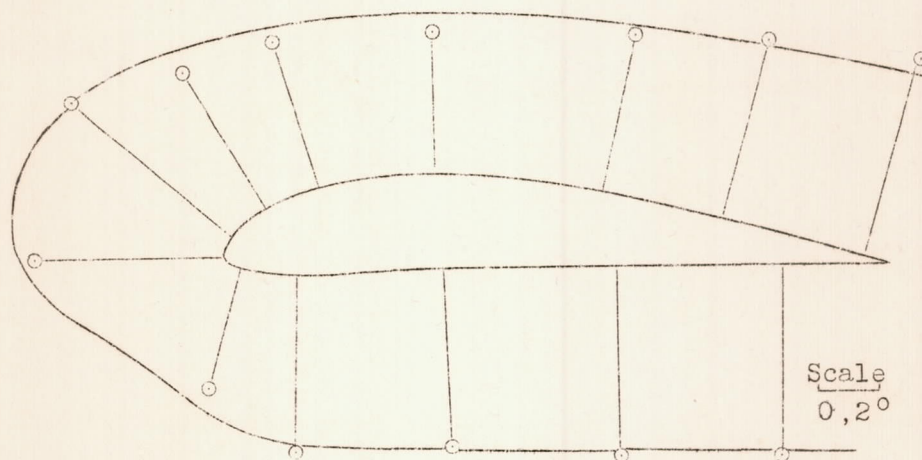


Figure 36.- Temperature record at $-3,1^\circ$ incidence. (wing)

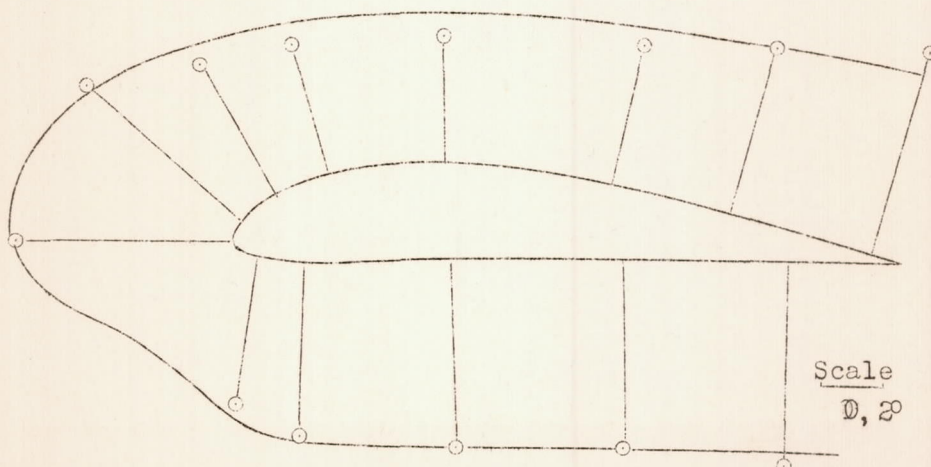


Figure 37.- Temperature record at 0° incidence. (wing)

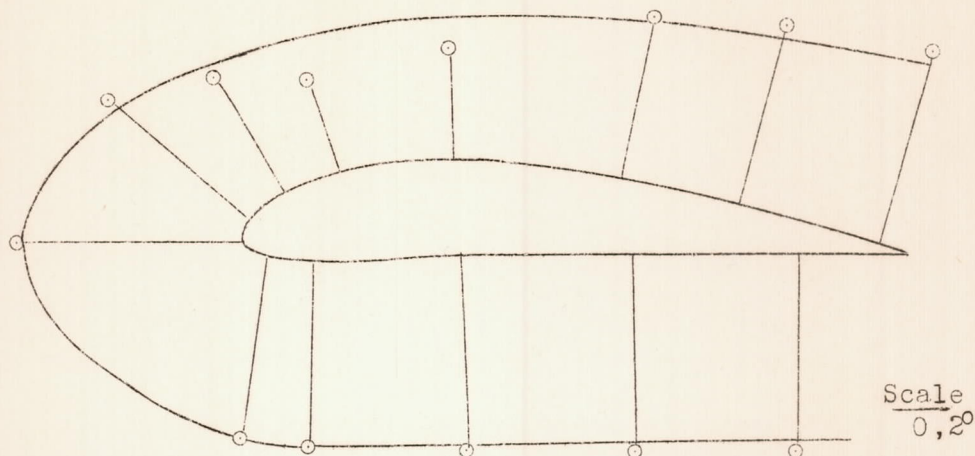


Figure 38.- Temperature record at 3,1° incidence. (wing)

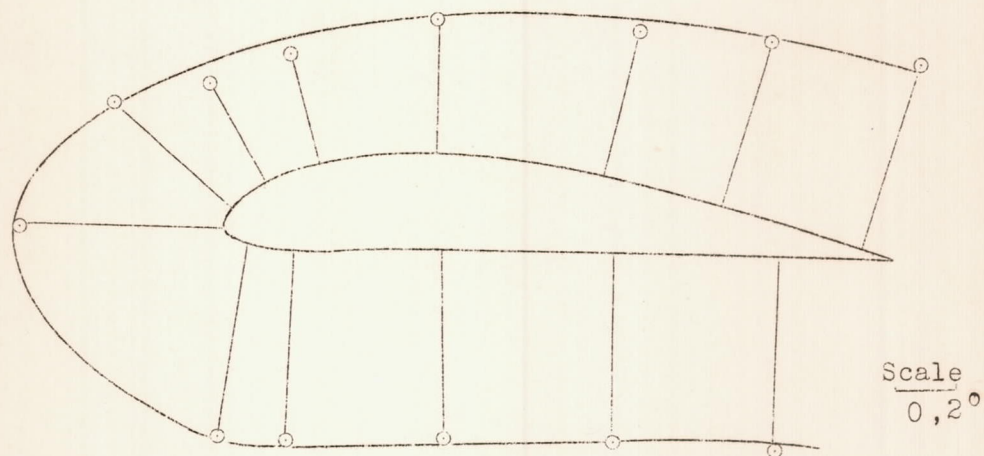


Figure 39.- Temperature record at 6,1° incidence. (wing)

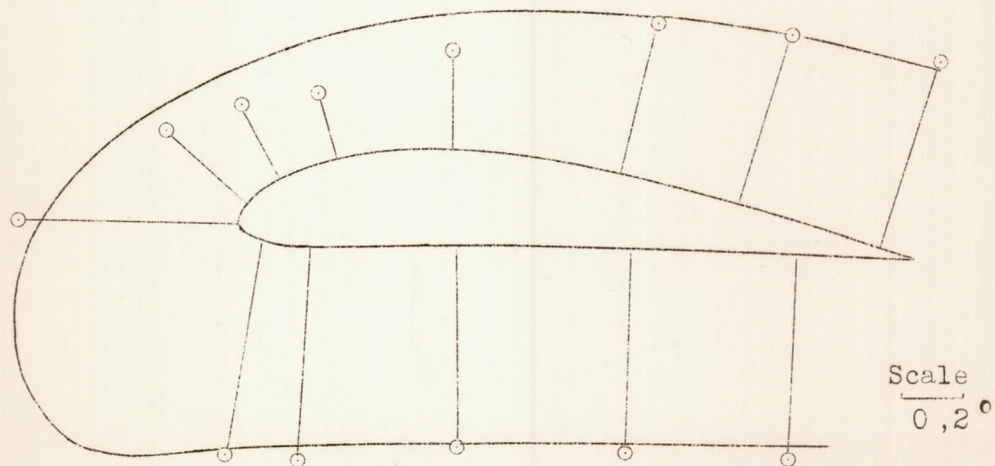


Figure 40.- Temperature record at 9,1° incidence. (wing)

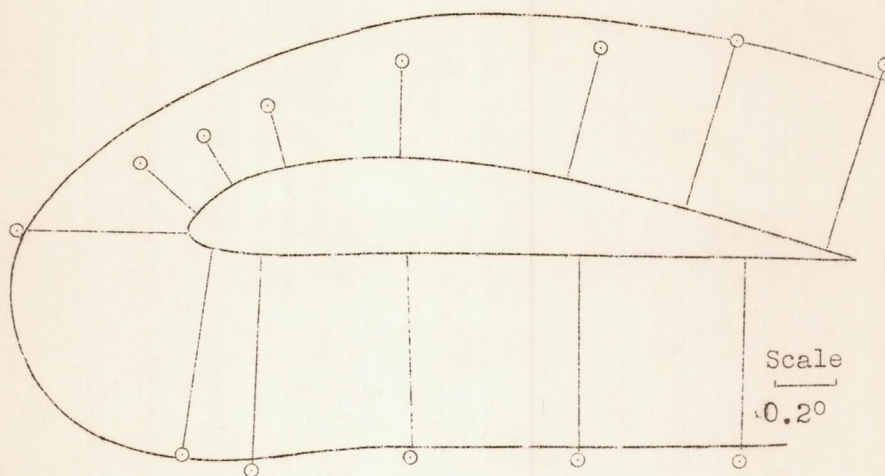


Figure 41.- Temperature record at 12.2° incidence (wing).

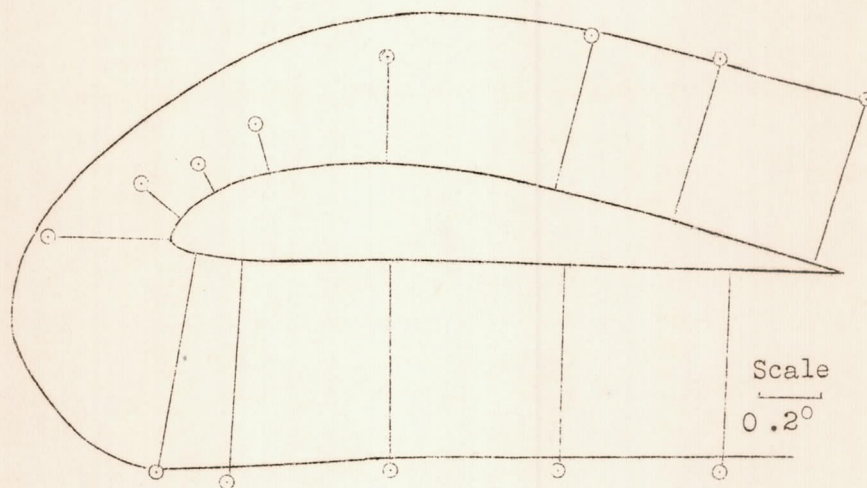


Figure 42.- Temperature record at 16.4° incidence (wing).

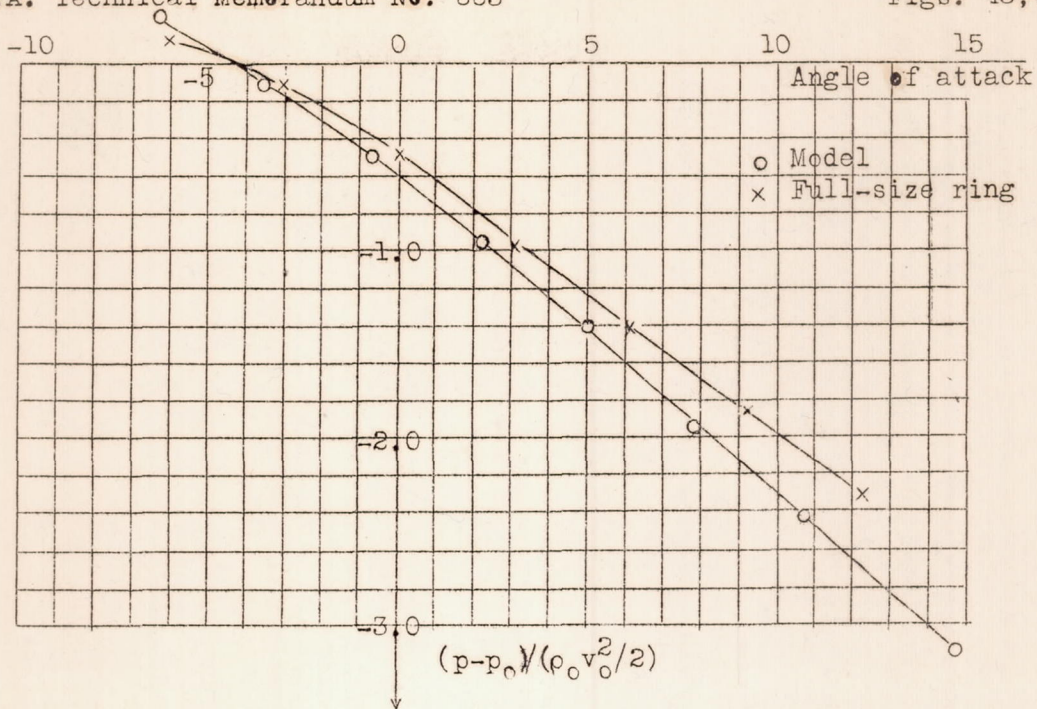


Fig. 43.- Comparison of results obtained on model and on wing at pressure tap No. 3.

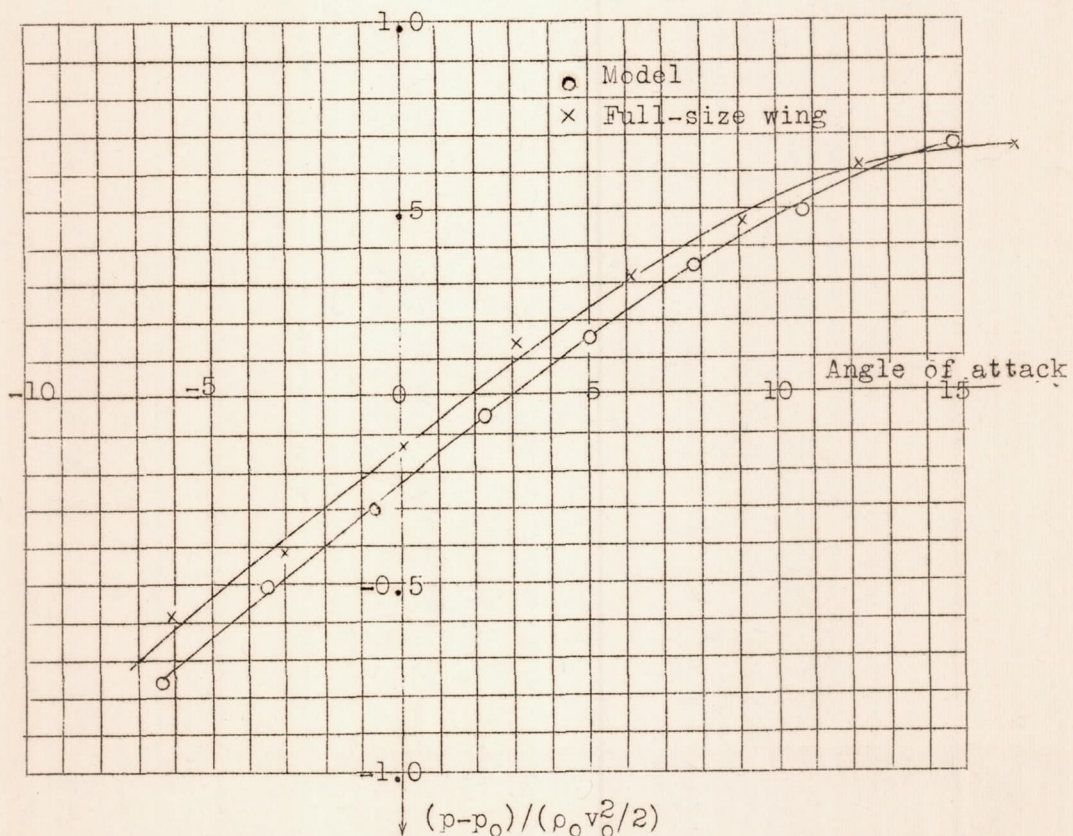


Fig. 44.- Comparison of results obtained with the model and the wing at pressure tap No. 12.